2021

Molecular Responses to Catastrophic Molting in a Wild Marine Mammal

Anna Keith
University of the Pacific

MOLECULAR RESPONSES TO CATASTROPHIC MOLTING IN A WILD MARINE MAMMAL

By

Anna Donaldson Keith

A Thesis Submitted to the

Graduate School

In Partial Fulfillment of the

Requirements for the Degree of

MASTER OF SCIENCE

College of the Pacific
Biological Sciences

University of the Pacific
Stockton, California

2021

MOLECULAR RESPONSES TO CATASTROPHIC MOLTING IN A WILD MARINE MAMMAL

By

Anna Donaldson Keith

APPROVED BY:

Thesis Advisor: Jane Khudyakov, Ph.D.

Committee Member: Craig Vierra, Ph.D.

Committee Member: Ryan Hill, Ph.D.

Department Chair: Eric Thomas, Ph.D.

MOLECULAR RESPONSES TO CATASTROPHIC MOLTING IN A WILD MARINE MAMMAL

By

Anna Donaldson Keith

DEDICATION

This thesis is dedicated to my friends and family who have supported me and believed in me through all my endeavors. To my parents, Michael and Rene Donaldson, who told me, even as a little girl, that I could be anything that I aspired to be. I would be nothing without your love and support. To my sister, Audrey Donaldson, my rock and my best friend, thank you for being a shoulder to cry on and helping me keep my mental sanity. To my wonderful loving husband, Jonathan Keith, I truly would not have been able to make it through my educational career without you by my side. You have encouraged and loved me every step of the way, especially when I needed it the most. I love you all very much and thank you for being my biggest cheerleaders.

ACKNOWLEDGMENTS

First and foremost, I would like to acknowledge my PI and advisor, Dr. Jane Khudyakov. I am incredibly thankful for your kindness and patience during the countless hours spent teaching and guiding me in laboratory research, data analyses, scientific writing, and field sampling. I would like to acknowledge our collaborators from the Crocker Lab at Sonoma State University and researchers from Point Reyes National Seashore and Año Nuevo State Reserve, without whom this project would not have been possible. I would like to acknowledge my committee members, professors, and mentors Dr. Ryan Hill and Dr. Craig Vierra. Thank you for teaching me about statistical analyses, mass spectrometry, field sampling, and aiding in the editing process. Additionally, thank you to my fellow graduate colleagues in Khudyakov Lab, Elizabeth, Lauren, and Jessica, for assisting in laboratory and collection procedures. Finally, I would like to thank the University of the Pacific for funding through my teaching assistantship and the Hunter Nahhas Fellowship Award.

MOLECULAR RESPONSES TO CATASTROPHIC MOLTING IN A WILD MARINE MAMMAL

Abstract

By Anna Donaldson Keith

University of the Pacific
2021

While most mammals shed their hair and skin either continuously or seasonally, northern elephant seals (*Mirounga angustirostris*) undergo an annual catastrophic molt, in which they shed their entire fur and underlying skin layer in the span of just three weeks. Due to the energetic and thermoregulatory constraints of molting and the large distances between their coastal rookeries and foraging grounds, elephant seals must remain on land and fast for the duration of their molt. Previous studies of molting northern elephant seals have examined endocrine and metabolic adjustments to fasting, but not the molecular processes underlying molting. We examined changes in the skin and underlying blubber tissues using histological, endocrine, and proteomic analyses during molting to provide a more in-depth understanding of the cellular mechanisms enabling rapid skin shedding and regeneration in this marine mammal. Shotgun proteome sequencing by LC-MS/MS identified 47,671 peptides and 573 protein groups in skin and outer blubber that were associated with lipid metabolism, protein processing in the endoplasmic reticulum, and collagen regulation. Label-free quantification and differential protein expression analyses identified 23 and 21 proteins that were differentially expressed during molting in the skin and outer blubber, respectively. Proteins downregulated over molting included those associated with inflammation, angiogenesis, and cellular proliferation, whereas proteins upregulated over molting included those associated with cytoskeletal remodeling,

collagen synthesis, and lipid metabolism. This suggests that rapid skin regeneration involves intensive protein synthesis and increased vascularization that may be supported by fatty acid substrates from underlying blubber tissue. These data provide insights into cellular and molecular mechanisms that govern unusually rapid skin regeneration in mammals, which may further understanding of disorders affecting the skin and hair of humans and other mammals.

TABLE OF CONTENTS

LIST OF TABLES

Table

LIST OF FIGURES

Figure

CHAPTER 1: INTRODUCTION

Skin, as the largest organ in the body, provides a protective barrier from physical damage, pathogen invasion, and metabolite loss (Eyerich et al., 2018). Understanding the metabolic and biological processes that drive tissue repair and replacement is essential to developing effective regenerative medicine. Several distinct processes are required for tissue regeneration, such as immune and inflammatory responses, activation of growth factors, initiation of cellular proliferation, and altered metabolism (Aurora et al., 2014). Although numerous genes and pathways have been associated with tissue regeneration, there are still gaps in our understanding of the cellular mechanisms that are essential for the regeneration of keratinous and epithelial tissues.

Skin and hair, feathers, and scales play an important role in protection, thermoregulation, coloration, locomotion, and reproduction in other mammals and birds and these structures must be regenerated regularly to maintain these functions (Chuong et al., 2002). Molting is the routine shedding of the outer covering of an animal, which often occurs on a seasonal or annual basis (Beltran et al., 2018). Despite its importance, molting is one of the most poorly studied life-history events, particularly in marine mammals. There are three main types of molting strategies in mammals: continuous shedding, a biannual molt, and an annual molt (Beltran et al., 2018). The most extreme and rapid form of mammalian skin shedding and regeneration is the catastrophic molt in monachid seals. Unlike other species, monachid seals, specifically northern elephant seals and monk seals, annually regenerate hair and skin cells in the span of roughly three weeks (Beltran et al., 2018).

Northern elephant seals spend the majority of their lifetime foraging in the mesopelagic zone of the Pacific Ocean, only coming onto land to give birth, breed, and molt (Le Boeuf, et al., 2000). Fur plays a minor role in thermoregulation in phocid seals, which have thick blubber layers for protection from the pressure and temperature differences that they face while forage diving to depths below 2000 meters (Le Boeuf, et al., 1994). However, the replacement of fur and skin during molting is an energetically demanding process and involves changes in skin perfusion that impair thermoregulation at sea, so elephant seals must haul out on land to complete this process (Le Boeuf et al., 1994). Due to the large distances between their foraging and haul out grounds, they must fast while they are on land. This has constrained molting to a period of 3-4 weeks once per year in elephant seals, whereas more coastal pinniped species can molt several times throughout the year over longer time periods (Le Boeuf, et al., 1994). During their annual catastrophic molt, elephant seals rapidly shed their entire pelage and epidermis (Le Boeuf, et al., 1994). No other mammal undergoes this rapid or extreme of a skin shedding and regeneration process while fasting. Therefore, northern elephant seals serve as a valuable model system to study rapid skin regeneration in mammals. Although we understand why they molt, the processes underlining how they molt are largely unknown.

Several studies have correlated stages of hair cycling to gene expression in terrestrial mammals (Beltran et al., 2018), but minimal research has explored this effect in a fasting marine mammal that undergoes this catastrophic molting. Changes in hormone levels and blubber and muscle protein and gene expression over fasting and in response to stress have been examined in fasting northern elephant seals; however, cellular and molecular changes in skin tissue during molting have not yet been examined (Yochem et al., 2008), (Khudyakov et al., 2015), (Jelincic et al., 2017), (Deyarmin et al., 2019), (Wright et al., 2020). The baseline variability in hormone

levels across life-history stages in northern elephant seals has previously been examined and corticosteroid hormones were found to increase over fasting in all age classes, with the largest spike in mid-molting (Jelincic et al., 2017), (Champagne et al., 2015). Additionally, thyroid hormones declined significantly over the molt haul out (Jelincic et al., 2017) (Champagne et al., 2015). This suggests that in addition to regulating fasting metabolism, corticosteroid and thyroid hormones may play a role in rapid skin shedding by regulating proteolysis, inflammation and protein synthesis, but the downstream targets of these hormones in skin tissue are currently unknown.

This study characterized changes in circulating corticosteroid and thyroid hormones, skin histology, and protein and gene expression in the skin and hypodermis between early and late molt in elephant seals, providing a more in-depth understanding of the endocrine, cellular, and molecular processes enabling rapid skin shedding and regeneration in a wild marine mammal. Understanding these processes could aid in skin and hair regenerative research pertaining to numerous skin shedding and hair loss disorders in other mammals, including humans, many of which have no known cures.

CHAPTER 2: STRUCTURAL CHANGES OF SKIN DURING CATASTROPHIC MOLTING

Introduction

Northern elephant seals undergo unusually rapid skin and hair regeneration while fasting, a process that involves significant morphological and cellular changes that have not previously been evaluated at the microscopic level. Correlations between stages of hair follicle activity and molting have been documented in other pinniped species, such as hooded seals, *Cystophora cristata*, (Ling et al., 2018), harbor seals, *Phoca vitulina*, and spotted seals, *Phoca largha* (Ashwell-Erickson et al., 1985), though, to our knowledge, none have examined the molting cycle of northern elephant seals.

Skin is composed of the epidermis, containing sweat glands and sebaceous glands, the dermis, containing collagen, elastin, and hair follicles, and the underlying subcutaneous adipose tissue, or hypodermis. The epidermis, consisting of predominantly keratinocytes and melanocytes, serves as the location of microbial and viral defense, regulating immune responses (Lai-Cheong et al, 2009). The epidermis is joined with the dermis via the dermal-epidermal junction, which links macromolecules of the epidermal keratinocytes with the collagen fibers in the underlying dermis. Abnormalities in this region often result in skin peeling, shedding, and blistering (Lai-Cheong et al, 2009). The dermis is composed of collagen and elastic fibers bound to glycoproteins, fibroblasts, dendritic cells, and sweat glands, which provide the thermoregulatory, secretory, and tactile capabilities of the skin. The hypodermis, composed of lipocytes, is the innermost layer of the skin and serves as an energy reserve, regulator of metabolism, and source of thermal insulation (Lai-Cheong et al, 2009).

Hair growth involves various stages of follicle and root development, including the anagen, catagen, and telogen phases. The anagen phase, or active growth phase, is a period of time when the hair root matrix stem cells are actively dividing (Alonso et al., 2006). The anagen phase is characterized by continued proliferation and differentiation of hair matrix stem cells toward the follicle base, keratinization of the inner root sheath, and tight packing of the hair shaft keratin filaments (Alonso et al., 2006). The catagen, or destruction phase, occurs due to a gradual decline in keratinocyte supply and ceased hair shaft differentiation. During this phase the hair follicle regresses through apoptosis of root sheath epithelial layers and separation of the dermal papilla (Alonso et al., 2006). The hair shaft becomes sealed, forming a club hair that remains anchored in the upper portion of the follicle. Following the catagen phase, the follicle enters the telogen, or resting phase (Alonso et al., 2006). The marked completion of telogen and transition back towards the anagen phase is through activation of the dermal papilla to produce a new hair shaft at the base of the follicle (Alonso et al., 2006). The dermal cells begin rapidly proliferating, causing a new follicle to form, leading to the removal or shedding of the previous club hairs (Alonso et al., 2006). Changes in the structure and activity of hair follicles, such as the ones described above, have not been examined during catastrophic molting in elephant seals. In this study, we conducted a histological comparison of skin samples collected from early and late molting adult female seals. Specifically, we examined and compared hair follicle activity, organization of structural proteins, cellular content, and density of skin layers between early and late stages of molting.

Figure 1. Early (<10% molted) and late (>90% molted) skin molting in northern elephant seals. Image Source: Khudyakov Lab, NMFS Permit No. 19108.

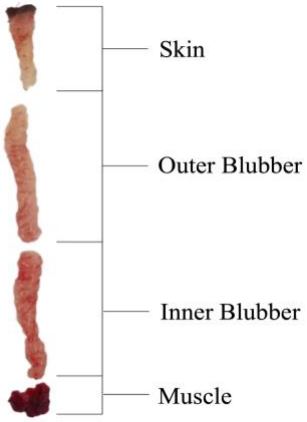

Figure 2. Skin, outer blubber, inner blubber, and muscle 6mm diameter tissue biopsy of northern elephant seals. Image Source: Khudyakov Lab, NMFS Permit No. 19108.

Methods

Study Subjects

Samples were collected from adult female northern elephant seals (n = 8) at Año Nuevo State Reserve (San Mateo County, CA) during the June 2020 molting period. All animal handling procedures were approved by Sonoma State University and University of the Pacific Institutional Animal Care and Use Committees and were conducted under National Marine

Fisheries Service marine mammal permit 19108. Early molt animals (n = 4) exhibited <10 % molting progress, whereas late molt animals were >90% molted (n = 4); (Fig. 1).

Sample Collection and Preparation

Study subjects were chemically immobilized with an initial intramuscular injection of ~1 mg/kg tiletamine-zolazepam HCl (Telazol, Fort Dodge Animal Health, Fort Dodge, IA, USA) and further sedated with intravenous doses of ketamine (0.25-1 mg/kg) (Fort Dodge Animal Health, Fort Dodge, IA, USA) as previously described (Fowler et al., 2016). Samples were collected from the posterior flank of the animals, after sterilizing skin with ethanol and iodine, using a 6.0 mm diameter biopsy punch (Miltex, USA) to extract skin and adipose tissues. Two samples were collected from each animal. One sample was rinsed in PBS and placed in 1% formalin on ice, while the other sample was blotted to remove red blood cells and flash frozen in liquid nitrogen after separating skin, outer blubber, and inner blubber layers (Fig. 2). Frozen samples were stored at -80°C upon return to the laboratory, and later used for RNA extraction (Chapter 5). After completion of sample collection, seals received rear flipper tags (Dalton, Oxon, UK) and were allowed to recover from anesthesia and resume normal activity.

All materials and reagents for histology were purchased from Thermo Fisher Scientific (USA) or VWR International (USA), unless otherwise stated. Paraffin embedding, sectioning, and hematoxylin-eosin staining were conducted according to Fischer et al., 2008.

Paraffin embedding. Formalin fixed tissue samples were stored at 4°C for 24 hours, after which they were rinsed 3 times for 30 min each in PBS, dehydrated in 70% ethanol, and stored at 4°C until further processing. Tissues were further dehydrated with 1 hour increments of 70%, 95%, and 100% ethanol. Dehydrated tissue samples were incubated at room temperature in three changes of 100% xylene (Merck, USA) for 1 hour each to eliminate lipids

and enable optimal paraffin binding. Defatted samples were embedded in paraffin through a series of gradual submersions in 60°C histoplast paraffin and mounted in 2.5 cm x 2.5 cm tissue molds made from silicone baking forms. Embedded tissue blocks were stored at 4°C for 12 hours. Hardened tissue paraffin blocks were removed from molds, trimmed, and attached to mounting cassettes. Tissue samples were mounted perpendicularly (n=4) and parallel (n=4) to the cassettes to obtain transverse and longitudinal sections.

Sectioning. Mounted blocks were loaded and sliced using a precision rotary microtome (AO Spencer No.820, American Optical Company, USA), at a 4° angle and 13 um thickness. Sections were flattened and floated onto microscope slides by submersion in a 45°C water bath and allowed to air-dry at room temperature for 12 hours. Slides were heated to 60°C for 15 minutes to ensure proper section binding. Half of the slides were used for hematoxylin-eosin staining, while the other half were used for phalloidin staining.

Hematoxylin-eosin staining. Slides were deparaffinized and rehydrated to allow for optimal stain binding. Slides were washed for 3 minute increments in the following solutions: xylene (2X), 1:1 xylene: 100% ethanol, 100% ethanol (2X), 95% ethanol, 70% ethanol, 50% ethanol, and PBS (3X). Slides were submerged in Hematoxylin for 2 minutes, rinsed with PBS, and stained with 1% Eosin Y Solution for 10 minutes. Dehydration was performed with 1 minute increments of: 95% ethanol (2X), 100% ethanol (2X), and xylene (2X). Slides were mounted with 100uL of S-Mounting Media with Acrylic. Hematoxylin- and eosin-stained slides were viewed using a Leica ICC50 W inverted microscope (Leica Microsystems Inc., USA).

Phalloidin staining. Slides were deparaffinized and rehydrated using the same protocol as above. Cellular membrane lipids were removed through permeabilization with 1% Triton X-100 in PBS for 15 minutes. Blocking of non-specific binding was achieved with 1% Bovine

Serum Albumin (BSA) in PBS for 45 minutes at room temperature. Staining was conducted using Alexa Fluor 568 Phalloidin (Life Technologies, USA) at 1:40 dilution in PBS with 1% BSA according to the manufacturer's protocol. Slides were stained for 45 minutes at room temperature, rinsed with PBS, and mounted with Invitrogen Antifade Gold Mounting Medium. Phalloidin-stained slides were viewed on Leica DMi8 Fluorescence Microscope (Leica Microsystems Inc., USA).

Statistical analyses. Morphological differences (number of follicles in distinct stages, club hairs, empty hair shafts, sebaceous glands, and epidermal thickness) between the early molt (n=4 samples, 42 total sections) and late molt (n=4 samples, 32 total sections) samples were evaluated using a Welch Two Sample t-test in R v4.2.0 (R Core Team, 2016; R Core Team, 2019) with differences considered significant at $p < 0.05$.

Results

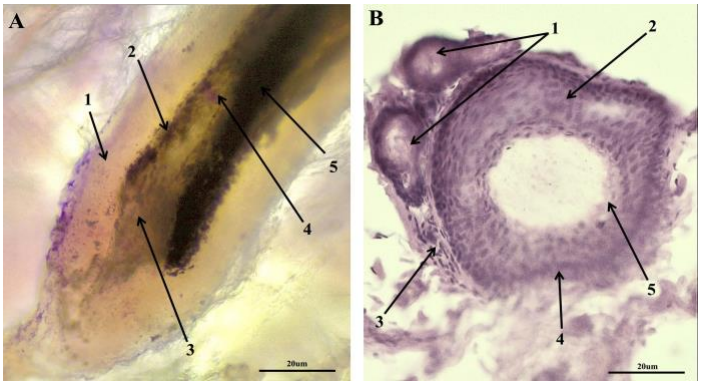

Figure 3. Hematoxylin and eosin stained longitudinal and transverse sections of elephant seal hair follicles. A) hair bulb longitudinal section, (a.1) dermal sheath, (a.2) cuticle, (a.3) dermal papilla, (a.4) medulla, (a.5) hair matrix. B) hair follicle transverse section, (b.1) sebaceous glands, (b.2) root sheath, (b.3) connective tissue, (b.4) glossy membrane, (b.5) cuticle.

Northern elephant seal skin and hair follicles displayed typical mammalian morphology with a core medulla surrounded by a keratinized cortex, and a highly keratinized cuticle on the outside of the hair (Fig. 3). Histological examinations of skin biopsies from the early molt samples showed significantly more follicles and hair roots within the catagen ($t=14.7$, $p=0.021$) and telogen ($t=10.3$, $p=0.043$) phases, whereas late molt elephant seals showed an enlargement and increased abundance of hair follicles within the anagen phase of hair growth ($t=10.26$, $p=0.0014$; Figs. 4,5,7). Additionally, the late molt skin samples exhibited an increase in abundance of sebaceous glands surrounding the anagen hair follicles ($t=11.9$, $p=0.023$; Fig. 8) and overall decrease in epidermal thickness compared to the early molt samples ($t=15.9$, $p=0.002$; Figs. 6,10). The early molt samples also exhibited an increased abundance of club hairs ($t=13.9$, $p=0.048$; Fig. 9) and reduction in empty hair shafts ($t=14.5$, $p=0.031$; Figs 11), a characteristic of the telogen growth phase, when compared to the late molt samples.

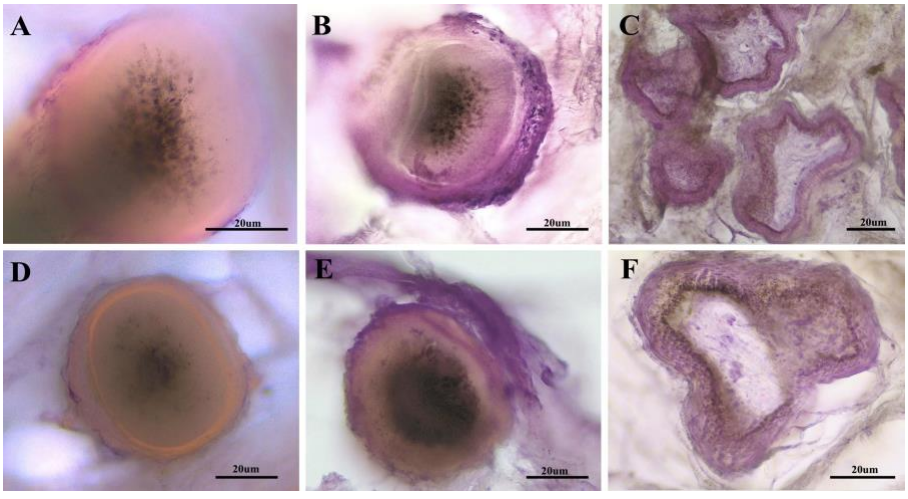

Figure 4. Hematoxylin and eosin stained sections of skin biopsies collected from northern elephant seals during early molt (b,c,e,f) and late molt (a,d). (a,d) Anagen phase (b,e) Catagen phase, and (c,f) Telogen phase.

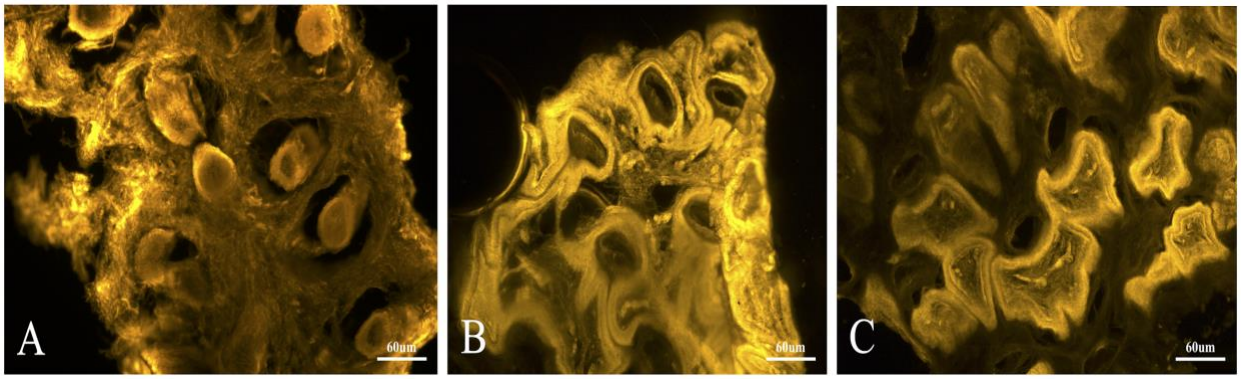

Figure 5. Phalloidin-stained sections of skin biopsies collected from northern elephant seals during early molt (b,c) and late molt (a). (a) Anagen phase (b) Catagen phase, and (c) Telogen phase.

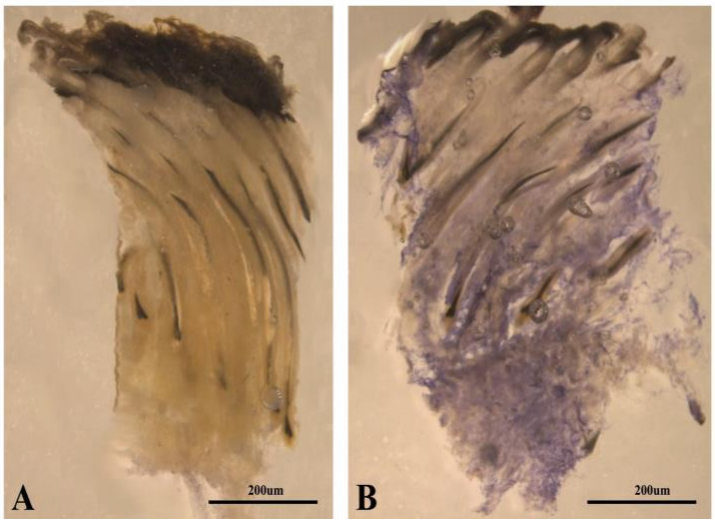

Figure 6. Hematoxylin- and eosin-stained longitudinal sections of skin biopsies collected from northern elephant seals during early molt (a) and late molt (b).

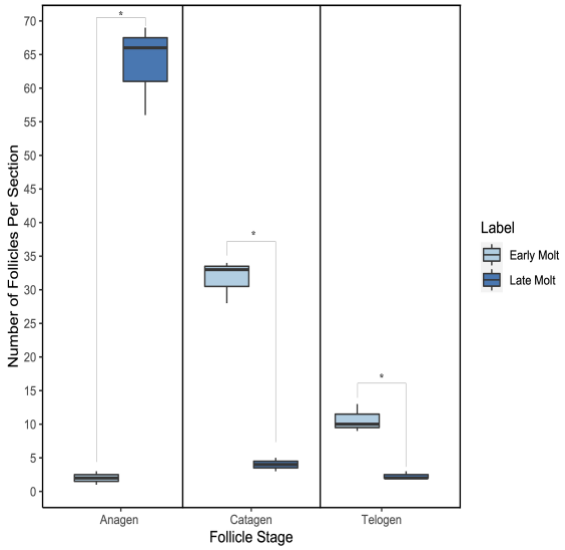

Figure 7. Box and whisker plots depicting average number of follicles per section in each follicular stage (anagen, catagen, and telogen) in early and late molt skin samples. *Denotes statistically significant differences between groups (Welch two-sample t-test, $p<0.05$).

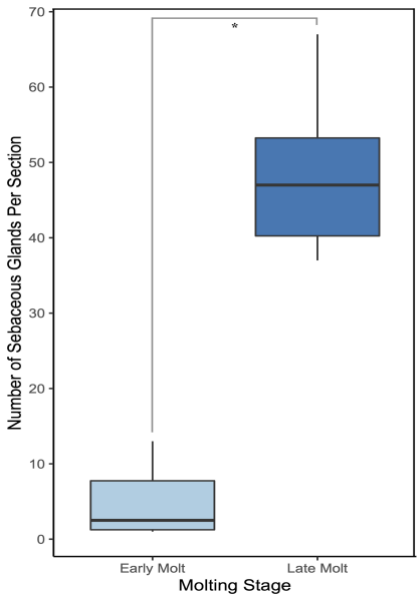

Figure 8. Box and whisker plot depicting average number of sebaceous glands per section in early and late molt skin samples. *Denotes statistically significant differences between groups ($p<0.05$).

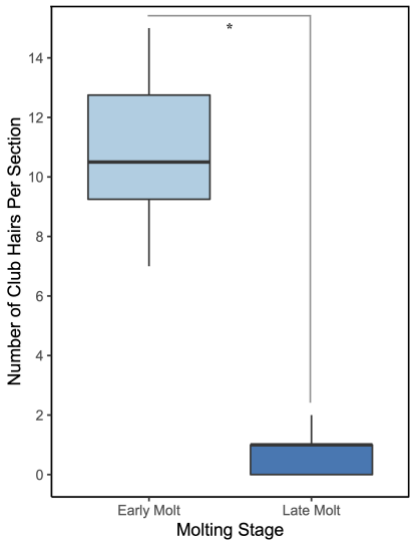

Figure 9. Box and whisker plot depicting average number of club hairs per section in early and late molt skin samples. *Denotes statistically significant differences between groups ($p<0.05$).

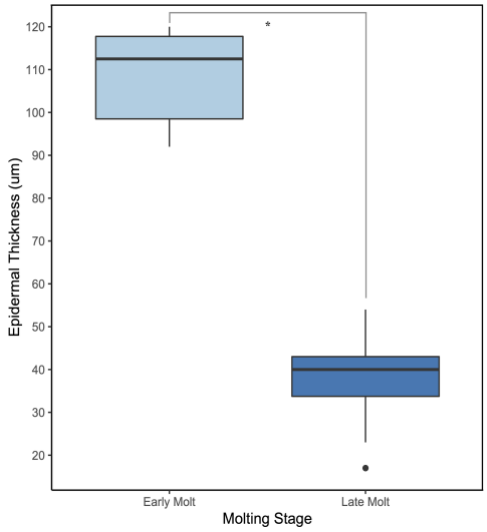

Figure 10. Box and whisker plot depicting average epidermal thickness per section in early and late molt skin samples. *Denotes statistically significant differences between groups ($p<0.05$).

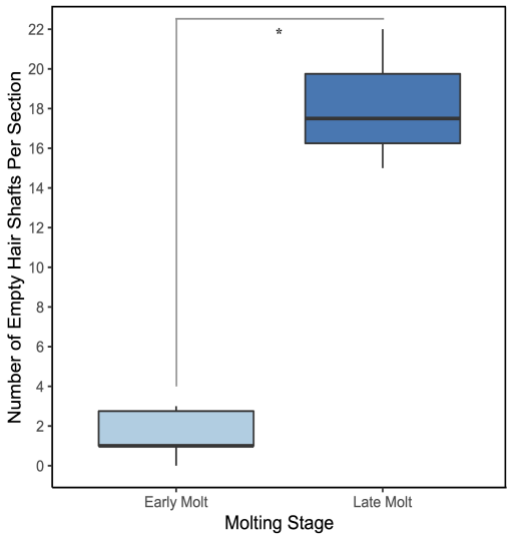

Figure 11. Box and whisker plot depicting average number of empty hair shafts per section in early and late molt skin samples. *Denotes statistically significant differences between groups ($p<0.05$).

Discussion

Histological examinations of skin biopsies from molting northern elephant seals identified changes in follicular activity, modifications in epidermal tissue thickness, sebaceous gland growth, and regulation of aging hair loss and regrowth, consistent with findings in other molting pinniped and mammalian species (Ling et al., 1970) (Ashwell-Erickson et al., 1985) (Ling et al., 2018).

The late molting skin samples showed a reduction in epidermal thickness and club hair abundance, which was expected during this rapid pelage shedding phase. Club hairs, or dead keratinized hairs, are formed during the catagen and telogen phases of the hair cycle in response to apoptosis of epithelial stem cells and regression of the hair shaft, as a result of lack in blood supply (Alonso et al., 2006). Expulsion of the club hairs from the hair follicle often marks the end of the hair cycle and transition towards the anagen growth phase of hair development.

At the beginning of the anagen growth phase, dermal cells are rapidly proliferating causing new follicle, hair, and sebaceous gland formation. In contrast to the early molting samples, an increase in abundance of sebaceous glands were present in the late molt samples. Sebaceous glands surround the hair follicles and provide lubrication to the skin and follicle through secretion of sebum. Sebum within pinniped species often assists with waterproofing and protection from oceanic conditions (Ling et al., 2018). Previous studies of other pinniped species have correlated both pelage reduction and lack of aquatic activity with decreased abundance of sebaceous glands (Ling et al., 1970) (Ashwell-Erickson et al., 1985) (Ling et al., 2018). The reduction in sebaceous glands during early molt correlates with a reduction in foraging activity during the early haul out, whereas later in the molt, the increased abundance of glands could be attributed to preparation for their upcoming forage migrations.

Alternatively, regression of sebaceous glands has previously been documented to play a key role in hair and skin homeostasis and regeneration in other mammalian species. Recent studies have implicated dysfunction or loss of sebaceous glands to destruction of hair follicles and ultimately hair loss (Neimann et al., 2012). Reductions in both sebaceous glands and sebum have also been correlated to onset of numerous hair and skin disorders, such as alopecia areata, keratosis pilaris, and atopic dermatitis (Neimann et al., 2012) (Gruber et al., 2015) (Shi et al., 2015). Reductions in sebaceous glands may be required for induction of epidermal death and sloughing during molting in seals. Together, these studies implicate sebaceous glands as important regulators of hair loss and regeneration, although the specific mechanisms are poorly understood and warrant further investigation.

In other mammal species, the transition time between club hair development, expulsion, and new hair follicle formation often takes months or even years (Paus et al., 1999), whereas in

northern elephant seals this process is accomplished within three weeks. This factor, once again, implicates this species as a valuable system for studying unusually rapid skin and hair regeneration.

CHAPTER 3: ENDOCRINE RESPONSES TO CATASTROPHIC MOLTING

Introduction

Alterations in hormones regulate life-history transitions in animals (Crespi et al., 2012; Finch et al., 1995) and changes in both corticosteroids and thyroid hormones have been observed during breeding and molting stages in northern elephant seals (Jelincic et al., 2017). In addition to regulating metabolism, corticosteroids have been associated with apoptosis, skin thinning, and suppression of inflammation, while thyroid hormones stimulate protein synthesis (Gruver-Yates et al., 2013; Kenessey et al., 2006). Corticosteroids, namely cortisol and aldosterone, have been shown to inhibit inflammatory pathways and promote collagen degradation and decomposition of connective tissue in previous skin regeneration and wound healing studies (Vidali et al, 2013; Boix et al., 2017). Thyroid hormones, such as free thyroxine (FT4) and total thyroxine (TT4), have been found to either increase hair loss or stimulate hair growth, depending on context, and to promote skin thinning and regulate epithelial cell proliferation in humans, implicating thyroid hormones as potential regulators of skin shedding and regeneration (Pascual et al., 2012; Antonini et al., 2013). Corticosteroids and thyroid hormones exert their effects in target cells by altering expression of genes involved in cellular proliferation, inflammation, and protein synthesis, suggesting that these hormones may play a role in skin and hair regeneration pathways in this marine mammal.

The baseline variability of corticosteroid and thyroid hormone levels across different life-history stages in northern elephant seals has previously been examined (Jelincic et. al., 2017). However, the potential roles of these specific hormones in skin and hair regeneration, via regulation of their target genes in the skin and outer blubber, have not been identified. Previous

studies have shown that levels of thyroid hormones decrease, whereas corticosteroids increase over molting, with a peak in mid-molt. Correlation of protein and gene expression in the skin and outer blubber with circulating hormone concentrations will provide an in-depth understanding into the endocrine, biochemical, and molecular mechanisms enabling this unusually rapid molting event. Concentration of corticosteroids, specifically cortisol and aldosterone in this study, are expected to be higher in the late molt samples relative to early molt samples, potentially to reduce inflammation and facilitate epithelial sloughing. Concentrations of thyroid hormones, total thyroxine (tT4) and free thyroxine (fT4), are expected to be highest in the early molt samples, during which epidermal cells are proliferating and differentiating and hair is being synthesized in the developing pelage (Beltran et al., 2018).

Methods

Study Subjects

Samples were collected from juvenile northern elephant seals (n = 6, 3 early molt and 3 late molt) at Point Reyes National Seashore (Marin County, CA) during the spring 2019 molting period and from adult female northern elephant seals (n = 6) at Año Nuevo State Reserve (San Mateo County, CA) during the summer 2017 molting period by methods previously described in Chapter 2.

Sample Collection and Preparation

Study subjects were chemically immobilized as previously described in Chapter 2. Samples were obtained from the extradural vein using an 18G, 3.2-inch spinal needle within 10 minutes of initial sedation. Samples were drawn directly into serum vacutainers (BD Franklin Lakes, NJ, USA). Blood samples were chilled on ice until returning to the laboratory. Serum was isolated by centrifuging at 3,000 x g for 15 minutes and stored at -80°C until further analysis.

Enzyme-linked immunosorbent assays (ELISA). ELISAs were used to measure serum concentrations of cortisol (11-CORHU-E01, Lot#192560, ALPCO, USA), aldosterone (11-AD2HU-E01, Lot#192490, ALPCO, USA), free thyroxine (FT4; 25-TT4HU-E01, Lot#RN-59682, ALPCO, USA), and total thyroxine (TT4; 25-FT4HU-E01, Lot#RN-59887, ALPCO, USA) following the manufacturer's standard protocols. Absorbances were read at 450nm using the Synergy H1 Hybrid Multi-Mode Reader (Agilent Technologies). GraphPad Prism9 (GraphPad, USA) was used to interpolate a standard curve (R^2=0.99, third-order polynomial fit). Statistically significant differences in hormone concentrations between early molt and late molt, in both juveniles and adult females, were calculated using a two-way ANOVA, with molting and age class as the two factors. Post-hoc tests were conducted between age classes using a t-test with Benjamini-Hochberg correction. Hormone concentrations were considered significantly different between molting groups at $p<0.05$.

ELISA validation for use in northern elephant seals was conducted following the standard methods for assay assessment of parallelism and accuracy (Andreasson et al., 2015). For parallelism assessment, serum samples with a known high concentration of each hormone were serially diluted 1:1 with the 0 concentration standard in each kit (1:1, 1:2, 1:4, 1:8, 1:18, 1:32). The measured hormone concentrations were then plotted against the theoretical calculated concentrations. For accuracy assessment using spike recovery, serum samples of known concentrations within the standard curve for each hormone were spiked with low, medium and high standards at a 1:1 standard to sample ratio. The obtained spiked concentrations were then used to calculate a percent recovery as followed:

$$\text{Recovery (\%)} = \left[\frac{\left(\begin{array}{c}\text{analyte concentration determined} \\ \text{in spiked sample}\end{array} \right) - \left(\begin{array}{c}\text{analyte concentration} \\ \text{in blank sample}\end{array} \right)}{\text{analyte concentration added to spiked sample}} \right] \times 100$$

A percent recovery between 80-120%, or a <20% error rate, validates the kit for use in non-model organisms and indicates that the kit is detecting the correct hormone without any potential matrix effects.

Results

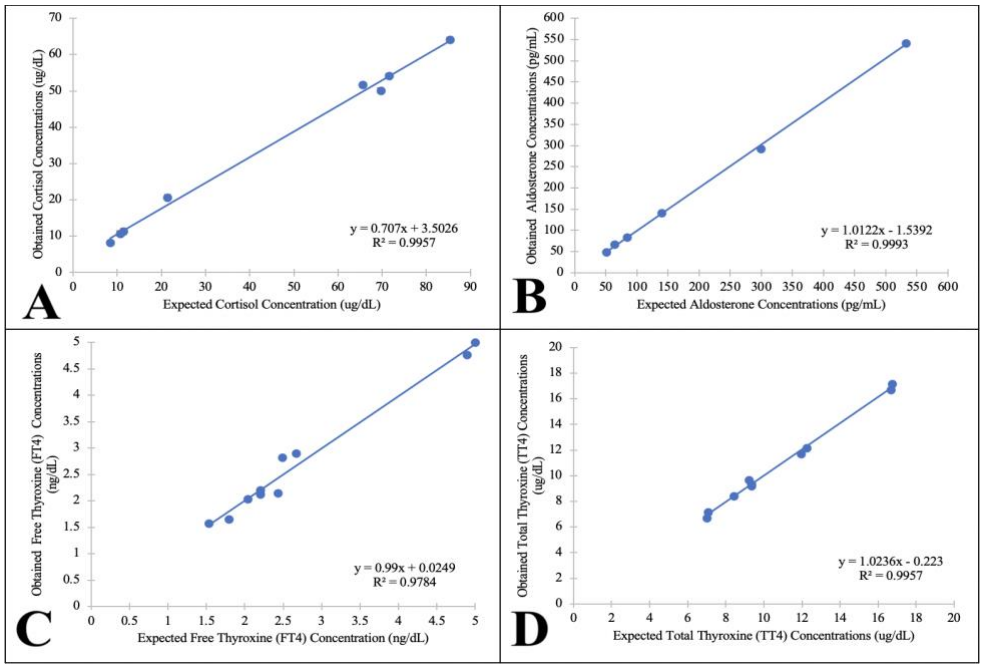

Figure 12. Parallelism of enzyme-linked immunosorbent assays (ELISAs) using northern elephant seal serum. Plots show regression of measured and expected hormone concentrations for A) cortisol, B) aldosterone, C) free thyroxine (FT4), D) total thyroxine (TT4).

Table 1
Spike Recovery Percentages for Enzyme-Linked Immunosorbent Assay (ELISA) Validations

Cortisol	Aldosterone	Free Thyroxine (FT4)	Total Thyroxine (TT4)
103.68 ± 4.86%	101.93 ± 12.65%	96.27 ± 11.70%	96.07 ± 4.24%

To assess parallelism, measured hormone concentrations were plotted linearly against predicted concentrations for each hormone and exhibited R^2 values within the acceptable range (>0.900) (Fig. 12). Parallelism of the serially diluted samples within the standard curve affirms the specificity of the assay and the lack of matrix effects. For spike recovery, each sample chosen yielded a percent recovery between 85-115%, when spiked with low, medium, and high standards (Table 1). Percent recoveries exhibited error rates of less than 15% indicating the ability of the assays to accurately detect high and low concentration of analyte within the serum matrix. These data confirmed that hormone concentrations could be accurately measured in elephant seal serum samples using these assays.

To understand the relationship between circulating corticosteroid and thyroid hormones and molting, ELISAs were used to detect cortisol, aldosterone, free thyroxine, and total thyroxine in early and late molt samples. Cortisol levels were significantly elevated during late molt, when compared to early molt seals, in both juveniles (early molt: 15.82±4.44ug/dL, late molt: 46.14±20.54ug/dL; $t = 2.48$, $p = 0.049$) and adult females (early molt: 6.58±4.67 ug/dL; late molt: 14.70±4.89 ug/dL; $t = 2.33$, $p = 0.048$) (Fig. 13). However, the juvenile samples exhibited significantly higher cortisol levels during late molting when compared to the adult females (juveniles: 46.14±20.54 ug/dL, adult females: 14.70±4.89 ug/dL; $t = 2.79$; $p = 0.041$) (Fig. 13). Aldosterone exhibited significant increases in concentration in late molt compared to early molt, in both juveniles (early molt: 298.94±94.67pg/mL; late molt: 594.03±127.98pg/mL; $t=2.47$; $p = 0.048$) and adult females (early molt: 191.97±94.2pg/mL; late molt: 620.47±84.97pg/mL; $t=4.83$; $p=0.008$) (Fig. 13). Aldosterone levels were not were not considered significantly different between age classes ($p>0.05$) (Fig. 13). Reductions in free thyroxine (FT4) were observed over molting in both juveniles (early molt: 20.44±0.32 μg/dL;

late molt: 9.05±0.45 ug/dL; t = 5.67; p = 0.005) and adult females (early molt: 12.08±0.17 ug/dL; late molt: 7.36±3.45 ug/dL; t = 4.19; p = 0.014), with higher levels in juveniles than females for both molting stages (juveniles: 20.44±0.32 ug/dL; adult females: 12.08±0.17 ug/dL; t = 18.09, p = 0.0001) and late molt (juveniles: 9.05±0.45 ug/dL; adult females: 7.36±3.45 ug/dL; t = 5.66, p = 0.005) (Fig. 13). Finally, reduction in total thyroxine (TT4) during late molting was observed in both juveniles (early molt: 1.41±0.32 ug/dL; late molt: 0.92±0.30 ug/dL; t = 2.80; p = 0.048) and adult females (early molt: 2.24±0.18 ug/dL; late molt: 1.84±0.29 ug/dL; t = 2.74; p = 0.041). However, there were no significant differences between age classes in either early molt (juveniles: 1.41±0.32 ug/dL; adult females: 2.24±0.18 ug/dL; t = 2.43, p = 0.059) or late molt (juveniles: 0.92±0.30 ug/dL; adult females: 1.84±0.29 ug/dL; t = 2.27, p = 0.058) (Fig. 13).

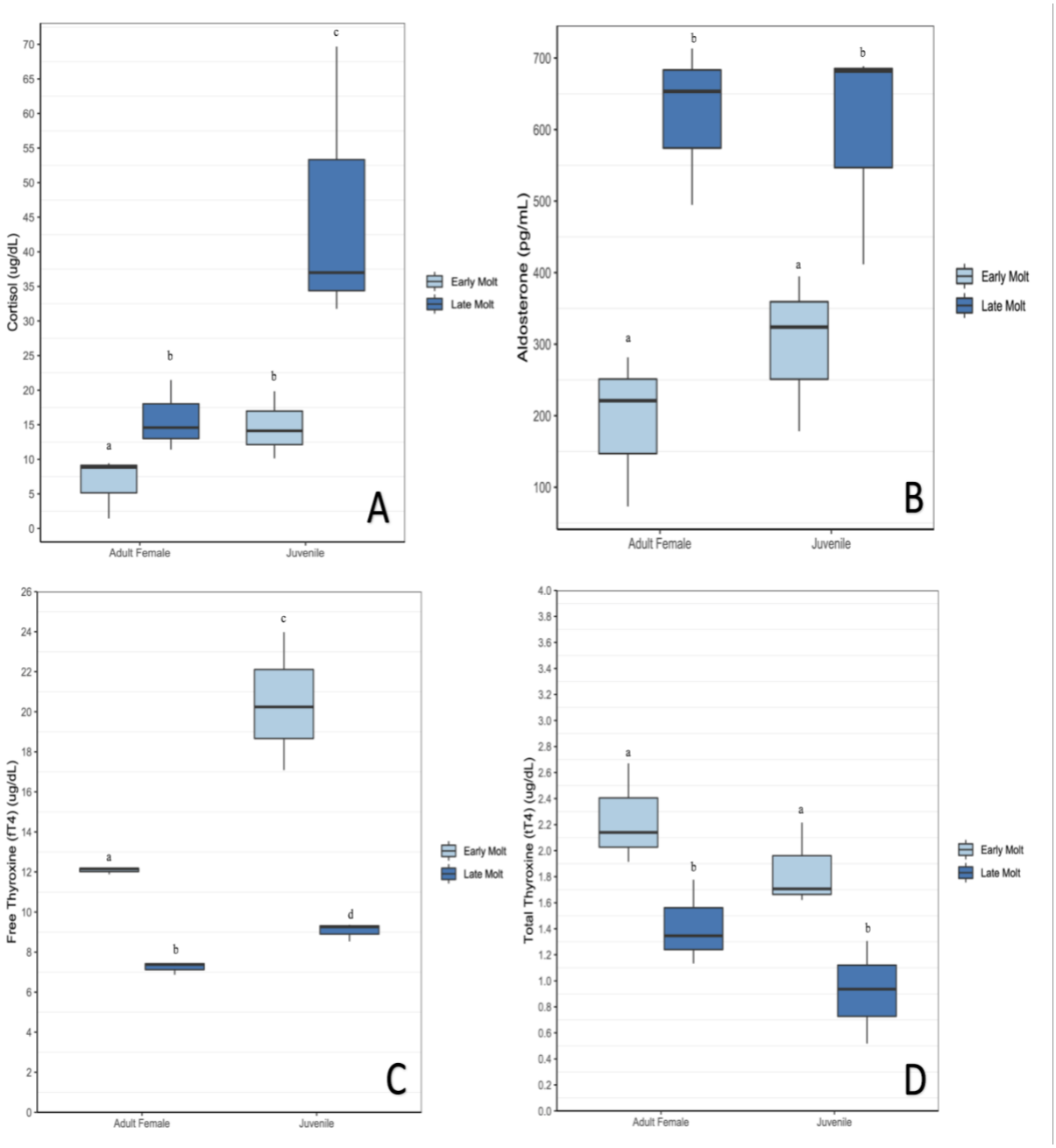

Figure 13. Variations in hormone concentrations between molting status (early v. late) and age class (adult female v. juvenile males and females): A) cortisol (n=12), B) aldosterone (n=12), C) free thyroxine (FT4) (n=12), D) total thyroxine (TT4) (n=12). Superscripts denote statistically significance difference between groups: early and late molting of juveniles and adult females ($p<0.05$).

Discussion

Increases in corticosteroids and significant reductions in thyroxine levels were seen over molting in both seal age classes, in agreement with findings of previous molting seal studies (Jelincic et al., 2017). Additionally, a strong agreement between both fT4 and tT4 confirms the reduction of thyroxine over molting. This suggests common regulation of these hormones over molting, regardless of sex or age class.

Skin and accompanying structures are not only responsive to circulating hormones, but they can also be a local source of hormonal secretion, inducing a wide variety of physiological responses (Chen et al., 2014). Corticosteroids, even in minute elevation, have been shown to impact metabolism, the immune system, inflammatory pathways, neurological functions, and organ homeostasis, including that of the skin (Chen et al., 2014). Significant upregulation of corticosteroids in the skin has been shown to inhibit proliferation and induce differentiation in epidermal keratinocytes (Chen et al., 2014). However, elevation of cortisol has also been linked to proliferation and inhibition of apoptosis in dermal fibroblasts and melanocytes and promotion of angiogenesis and vascular permeability to granulocytes (Chen et al., 2014), suggesting that the effects of cortisol are cell type-specific, but may regulate extracellular matrix formation and aid in synthesis of cells responsible for developing epidermal and dermal tissues. In previous studies, elevated corticosteroids have been shown to induce hair growth and synthesis in other organisms (Paus et al., 1994). Aldosterone, predominantly known for its osmoregulatory role, is elevated over all fasting periods in seals and may play a yet-unknown role in fasting metabolism and even molting (Jelincic et al., 2017). Aldosterone has been shown to stimulate collagen and elastin deposition, increase epidermal thickness, and induce inflammatory responses in human

skin studies (Boix et al., 2017), suggesting that this hormone, in addition to cortisol, may play a role in skin and hair regeneration over the molting process in phocid seals as well.

Thyroid hormones, additionally, exhibit tissue-specific functionality through regulation of metabolic, digestive, cardiovascular, and immune pathways. Several studies have implicated that thyroid hormones are essential for skin homeostasis through alteration of collagen deposition, epidermal proliferation and differentiation, and inflammatory pathways (Antonini et al., 2013). The reported effects of elevated thyroid hormones (hyperthyroidism) in human skin are complex. However, numerous studies have shown that excess thyroid hormones result in skin thinning, reduced keratinocyte proliferation, and induction of apoptosis of hair follicle cells (Antonini et al., 2013; Grachtchouk et al., 2011; Tiede et al., 2010). Additionally, upregulation of thyroid hormone results in a decrease in the growth of dermal fibroblasts (Moeller et al., 2005) and suppression of integrins involved in cell membrane adhesion (Tomic-Canic et al., 2008). These findings suggest that thyroid hormones may be involved in keratinocyte and hair follicle degradation, which is seen during the skin shedding, early phase of molting.

Higher levels of thyroid hormones during early molt may promote inflammation, extracellular degradation and hair loss which enable skin shedding. In contrast, higher levels of cortisol and aldosterone in late molt may promote angiogenesis, extracellular matrix synthesis, and hair growth that are necessary to generate new pelage. These data were consistent with previous studies showing elevation in corticosteroids and reduction in thyroid hormone levels over molting, suggesting that these changes may play a role in regulation of molting. However, the tissue-specific effects of these hormones via their receptors should be confirmed in future studies.

CHAPTER 4: PROTEOME DYNAMICS DURING CATASTROPHIC MOLTING

Introduction

Tissue regeneration (e.g. during wound healing) is a relatively conserved process among different species and encompasses physiological mechanisms such as inflammation, cellular proliferation, and extracellular matrix remodeling (Takeo et al., 2015). Mammalian skin is composed of the epidermis, containing epithelial cells, hair follicles, and sebaceous glands, and the dermis, consisting of fibroblasts, blood vessels, immune cells, sensory nerves, and adipocytes regulating nutrient supply from underlying adipose tissue (Fig. 14) (Dekoninck et al., 2019). The inflammatory phase of skin regeneration is characterized by increased migration of immune, dermal and epidermal cells into the dying tissue. Macrophages produce growth factors, such as transforming growth factors (TGFs), inflammatory cytokines, interleukins (ILs), and tumor necrosis factors (TNFs), increasing the abundance of fibroblasts (Fig. 14) (Dekoninck et al., 2019). During the proliferation phase of wound healing, keratinocytes, fibroblasts and endothelial cells proliferate and contribute to growth of new tissue, angiogenesis, collagen deposition, granular tissue formation, and epithelial cell migration (Fig. 14) (Dekoninck et al., 2019). The final phase of tissue regeneration is the extracellular matrix remodeling phase, during which granulation tissue develops and fibroblasts stimulate the production of collagen, giving the new tissue its strength and structure (Fig. 14) (Dekoninck et al., 2019). Although numerous genes and pathways have been associated with tissue regeneration, there are still gaps in our understanding of which factors are essential for the regeneration of keratinous and epithelial tissues.

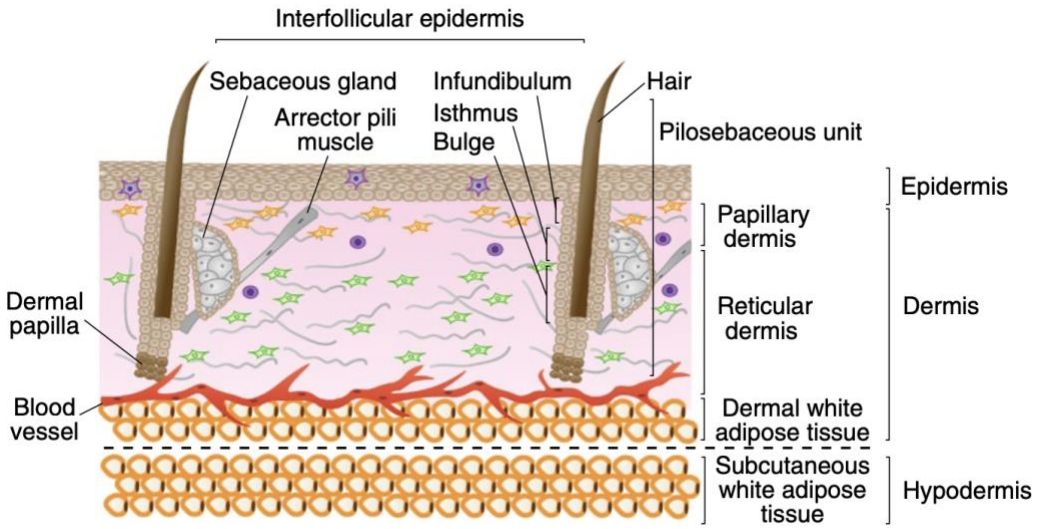

Figure 14. Illustration of skin and adipose structural components essential for tissue regeneration. Image obtained from (Dekoninck et al., 2019).

Several studies have correlated stages of hair cycling to protein and gene expression in terrestrial mammals (Wu et al., 2008; Zimova et al., 2018), however, similar molecular studies have not been conducted in a fasting marine mammal undergoing catastrophic molting. Previous studies of molting northern elephant seals have examined changes in protein and gene expression in response to fasting and stress challenges, but not the molecular processes underlying molting (Khudyakov et al., 2015; Deyarmin et al., 2019; Wright et al., 2020). To our knowledge, this is the first study to analyze a skin proteome from any life history stage of northern elephant seals, in addition to being the first proteomic analysis of catastrophic molting.

We used shotgun proteomics, a powerful approach for rapidly identifying proteins in non-model organisms, to examine the cellular mechanisms enabling rapid skin shedding and regeneration in this marine mammal. Historically, genomic sequencing has been constrained to model organisms, due to their ease of manipulation in laboratory settings (Oliver et al., 2016). Although large abundances of genomic model organism studies exist, their accurate

representation of biodiversity across species is limited (Russell et al., 2017). Genomic studies of non-model organisms provide answers to numerous biological questions previously unattainable through model organism studies (Russell et a., 2017). However, advancements in non-model studies have progressed at a much slower pace due to limited comparative and functional datasets, until recently (Russell et al., 2017). Shotgun proteomics in non-model organisms allows for identification of large protein datasets and changes in protein expression even in the absence of sequenced genomes (Deyarmin et al., 2019). Proteins upregulated in skin and blubber during molting and their known functions in other organisms can provide insights into the regulatory and cross-tissue communication mechanisms responsible for rapid skin regeneration. Thus, use of this approach may provide insights into the cellular and molecular processes underlying molting in this "non-model model" organism of catastrophic molting.

Skin regeneration involves intensive protein synthesis, activation of inflammatory pathways, and modifications in structural proteins (Dekoninck et al., 2019). We expect to see upregulations of proteins associated with proteolysis and inflammatory proteins in the early molt skin samples, as the seals are undergoing rapid skin shedding. In contrast, we expect proteins associated with protein synthesis, increased vascularization, and extracellular matrix remodeling to be upregulated during late molt, in order to support rapid skin growth and functional development. Blubber tissue is the intermediary for nutrients and metabolites between the skin and internal organs, as well as the source of adipokines and growth factors that may play a role in regulating metabolism and molting in skin. Thus, we expect upregulation of blubber proteins involved in vascularization, lipid mobilization, regulation of fasting metabolism, and growth factors supporting proliferation of epidermal cells over the molting period.

Methods

Sample Collection

Samples were collected from juvenile northern elephant seals (n=6) at Point Reyes National Seashore (Marin County, CA) during the spring 2019 molting period by methods previously described in Chapter 2. Biopsies were collected from the posterior flank of each animal using a 6.0- mm diameter biopsy punch (Miltex, USA). Skin and outer blubber were separated by dissection, placed in cryovials, flash-frozen, and stored in liquid nitrogen until return to the laboratory. Samples were stored at -80°C until further processing. At the conclusion of sampling, seals received rear flipper tags (Dalton, Oxon, UK) and were allowed to recover from anesthesia and resume normal activity.

Sample Preparation

Protein isolation and denaturation. Skin and blubber samples were homogenized by bead beating in Trizol (Ambion, USA; ~50mg tissue per 1.0 mL) or Qiazol (Qiagen, USA; ~100mg tissue per 1.0 mL), respectively, using 2.0-mL tubes pre-filled with 2.4-mm metal beads (Fisher Scientific, USA) using the Bullet Blender Storm 24 (Next Advance, USA; Speed 12, two 2-minute cycles). Nucleic acids were removed using chloroform phase extraction according to manufacturers' protocols (12,000g x 15 min at 4°C). Proteins remaining in the organic phase were precipitated using 100% isopropanol and pellets were washed using 0.3 M guanidine hydrochloride in 95% ethanol. Protein pellets were solubilized in Denaturing Solution (8M urea, 5mM dithiothreitol (DTT), 1% w/v sodium deoxycholate (SDC) in 50mM ammonium bicarbonate (AmBiC)) by vortexing for 2 hours at room temperature and denatured at 37°C for 1 hour.

Alkylation, quantification, and digestion. Proteins were alkylated with 15mM iodoacetamide (IAA) for 30 minutes in the dark at room temperature and quenched with 5mM

DTT for inactivation and removal of unused IAA. Urea concentrations were reduced to < 1M by dilution with 50mM AmBiC. Protein concentrations were obtained using the bicinchoninic acid (BCA) assay (Thermo Scientific, USA). Samples were assayed in duplicate (mean CV = 1.74%, SD=1.62) and GraphPad Prism9 (GraphPad, USA) was used to interpolate the standard curve (R^2=0.99, quadratic second-order polynomial fit). The same amount of protein from each sample (100ug) was digested using Trypsin Protease MS Grade (Thermo Scientific, USA) at a 1:50 ug trypsin to protein ratio for 16 hours at 37°C. Trifluoroacetic acid (TFA) was added to a final concentration of 0.5% v/v to acidify the protein samples to pH <2 to inactivate trypsin and precipitate SDC. SDC was removed by centrifugation (14,000g x 10 min at 4°C) and extraction of the supernatant.

Desalting, lyophilization, and dilution. Digested peptides were lyophilized and desalted using Pierce Peptide Desalting Spin Columns following the manufacturer's protocol (Thermo Scientific, USA). Eluted desalted peptides were lyophilized and resuspended in 0.1% formic acid in LC-MS grade water. The Pierce Quantitative Colorimetric Peptide Assay (Thermo Scientific, USA) was used for final peptide quantification. Samples were assayed in duplicate (mean CV = 1.43%, SD=1.03) and GraphPad Prism9 (GraphPad, USA) was used to interpolate the standard curve (R^2=0.99, third-order polynomial fit). Samples were diluted to a final concentration of 200ng/uL prior to sequencing.

LC-MS/MS. Each sample was run in three technical replicates. For each run, 5 μL of sample was loop injected onto a reversed-phase trap column (Acclaim PepMap 100 C18 LC column; 75 μm i.d. x 2 cm, 3μm particle size, 100 A pore size, Thermo Fisher Scientific, USA) by a Dionex Ultimate 3000 autosampler. Peptides were eluted onto a reversed-phase analytical column set at 35°C for HPLC (EASY-SprayTM C18 LC column; 75 μm i.d. × 15 cm, 100 A,

Thermo Fisher Scientific, USA). Solvents A and B were water and acetonitrile (both with 0.1% formic acid), respectively. During the chromatographic run, solvent B was used as follows: 3% for 5 min, 3%–28% for 75 min, 28%–45% for 25 min, 45%–95% for 5 min, 95% for 5 min, return to 3% for 5 min, followed by 2% for 25 min. Flow rates were held at 300 nl/min with each sequencing run set to 140 minutes. Mass spectrometry analysis was performed using Orbitrap Fusion™ Tribrid™ mass spectrometer equipped with an EASY-Spray™ ion source (Thermo Fisher Scientific, USA) operated in a data dependent acquisition (DDA) manner by Xcalibur 4.0 software (Thermo Fisher Scientific, USA. MS1 spectra were resolved by the orbitrap with resolution of 120,000, scan range of 200-1400 m/z, RF lens of 60%, AGC target of 1.0e6, and max injection time of 50 ms. Precursor ions selected using DDA were isolated by quadrupole and fragmented using HCD with collision energy of 28% ± 3%. MS2 product ions were also resolved by the orbitrap with resolution of 30,000, AGC target of 5.0e5, first mass of 100 m/z, and max injection of 150 ms.

MS/MS data analysis. Protein identification and label-free quantification were performed using MaxQuant v1.6.14.0 with default settings. Skin and blubber samples were analyzed separately. Technical replicates for each biological replicate ("experiment") were analyzed as part of the same experiment; the median abundance values for 3 technical replicates were reported. The "match between runs" (MBR) function was enabled with a matching time window of 0.7 min and alignment time window of 20 min. Database search was conducted using MaxQuant's Andromeda search engine against the UniProtKB Caniformia database containing 511,086 entries (Taxonomy ID: 379584, downloaded on August 3, 2020) and a MaxQuant contaminant database. Carbamidomethylation (C) was selected as a fixed modification and oxidation (M) and deamidation (NQ) were selected as variable modifications; a maximum of 3

modifications per peptide were allowed. False discovery rate was determined by searching the reversed Caniformia and contaminant databases. Only hits below 1% FDR were retained for further analyses; hits to contaminant or reversed databases were removed. Protein quantification was conducted based on precursor ion intensity using the MaxLFQ algorithm in MaxQuant. Both razor and unique peptides were used for quantification and the minimum ratio for quantification was 2. FastLFQ normalization was used and the "stabilize large LFQ ratios" and "require MS/MS for LFQ comparisons" options were checked.

Differential protein expression analyses. LFQ abundance values were log2-transformed. Proteins that had two or more missing values per sample group were removed. Remaining missing values (max one per sample group) were imputed using the llsImpute function in the pcaMethods Bioconductor package (Stacklies et al., 2007) with k = 150 in R v4.2.0 (R Core Team, 2016; R Core Team, 2019). Differential expression analyses were conducted using limma v3.44.3 Bioconductor package (Ritchie et al., 2015). Proteins with abundances that differed by more than 20% between groups (above 1.2-fold and below 0.8-fold) were considered differentially expressed. Protein expression was summarized in a heatmap using the pheatmap ggplot2 R package v.3.3.3 (Kolde, 2019) with complete clustering of rows by euclidean distance. Functional enrichment analysis of differentially expressed proteins was conducted using Enrichr tool (Chen et al., 2013; Kuleshov et al., 2016) and the human WikiPathways 2019 database (Slenter et al., 2018). Pathways were considered enriched relative to the human proteome background at adjusted $p < 0.05$.

Results

In this study, we characterized the outer blubber and skin proteomes of six juvenile northern elephant seals during early and late molting. The proteome metrics for skin and blubber in juvenile northern elephant seals are described in Table 2.

Table 2
Metrics of Skin and Outer Blubber Proteomes Over Molting

	Skin	Blubber
MS/MS Spectra	856,707	408,044
Peptide Spectra Matches (PSM)	25,439	22,232
UnitProt SwissProt Identified Proteins	8,010	2,096
Protein Groups	389	184
Proteins downregulated over molting [fc < 0.8-fold]	7	8
Proteins upregulated over molting [fc > 1.2-fold]	16	13

Note. Differentially expressed proteins exhibited a fold change (fc) of greater than 20% between molting groups.

Molting Skin Proteome

We identified 8,010 proteins in 389 protein groups in elephant seal skin tissue. Functional annotation of the molting skin proteome identified 11 KEGG pathways that were enriched (adj. $p < 0.05$) in elephant seal skin relative to the human proteome. Enriched pathways of interest included ribosomal proteins (n=5 proteins), protein processing in the endoplasmic reticulum (n=5), lipid metabolism (n=4), and collagen regulation (n=3). Sixteen proteins were upregulated, while seven were downregulated over molting in elephant seal skin. The magnitude and significance of protein expression changes between samples are presented in Fig. 15a. Manual UniProt and Pubmed database searches were used to infer the functions of DEPs and

their potential roles in skin regeneration. DEP identifications and their known functions in other organisms are listed in Tables 3 and 4. Proteins downregulated over molting in the skin tissue included those with known associations with inflammation, cell proliferation, lipid mobilization, and cytoskeletal remodeling. Proteins upregulated over molting in the skin tissue included those with known functions in collagen synthesis and epithelial integrity, lipid mobilization and metabolism, cytoskeletal remodeling, and protein synthesis and processing in the endoplasmic reticulum.

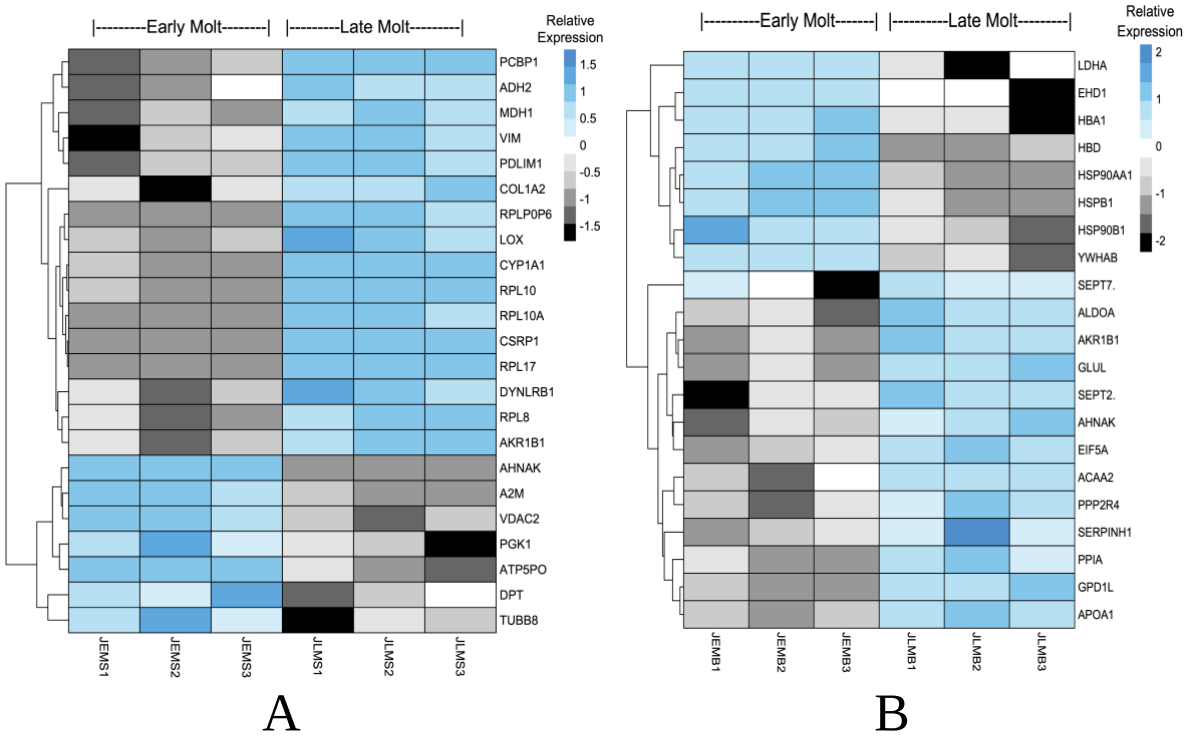

Figure 15. Heatmaps depicting differences in protein expression between early and late molting in skin (a) and outer blubber (b) samples. The proteins shown had abundances that differed by more than 20% between groups and are clustered by expression level (Euclidean distance). Relative expression is depicted by gradients of blue (upregulated over molting), white (no change), and black (downregulated over molting).

Table 3
Skin Proteins Upregulated by 1.2-Fold or Higher Over Molting

Gene Symbol	Uniprot Accession	Protein ID	Adjusted P value	Log2 Fold Change	General Functions
VIM	P08670	Vimentin	7.74E-04	5.05	Collagen Fibril Organization
CSRP1	P21291	Cysteine and glycine-rich protein 1	7.00E-10	5.45	Cytoskeletal Organization
CYP1A1	P04798	Cytochrome P450 1A1	1.50E-07	5.12	Fatty Acid Metabolism
RPL17	P18621	60S ribosomal protein L17	7.14E-07	3.26	Ribosomal Protein
RPL10	P27635	60S ribosomal protein L10	5.31E-06	3.21	Ribosomal Protein
RPL10A	P62906	60S ribosomal protein L10a	5.31E-06	2.73	Ribosomal Protein
RPL8	P62917	60S ribosomal protein L8	2.86E-04	2.27	Ribosomal Protein
MDH1	P40925	Malate dehydrogenase, cytoplasmic	1.92E-04	1.92	Malate Metabolic Process
PDLIM1	O00151	PDZ and LIM domain protein 1	3.37E-04	1.81	Cytoskeletal Organization
PCBP1	Q15365	Poly(rC)-binding protein 1	1.92E-04	1.83	Nucleic Acid Binding Protein
DYNLRB1	Q9NP97	Dynein light chain roadblock-type 1	1.15E-03	1.82	Cytoskeletal Organization
AKR1B1	P15121	Aldo-keto reductase family 1 member B1	7.74E-04	1.66	Glucose Metabolism
COL1A2	P08123	Collagen alpha-2(I) chain	1.39E-02	1.01	Collagen Fibril Organization
RPLP0P6	Q8NHW5	60S acidic ribosomal protein	2.42E-04	0.71	Ribosomal Protein
LOX	P28300	Protein-lysine 6-oxidase	5.84E-04	0.48	Collagen Fibril Organization

Table 4
Skin Proteins Downregulated by 0.8-Fold or More Over Molting

Gene Symbol	Uniprot Accession	Protein ID	Adjusted P value	Log2 Fold Change	General Functions
DPT	P19427	Dermatopontin	1.14E-02	-0.41	Collagen Fibril Organization
TUBB8	Q3ZCM7	Tubulin beta-8 chain	4.39E-03	-0.42	Microtubule Protein
AHNAK	Q09666	Neuroblast differentiation-associated protein AHNAK	9.84E-05	-0.67	Neuronal Cell Differentiation
PGK1	P00558	Phosphoglycerate kinase 1	5.12E-03	-0.67	Glycolytic Enzyme
ATP5PO	P48047	ATP synthase subunit O, mitochondrial	1.70E-03	-1.22	Mitochondrial ATP Synthesis
A2M	P01023	Alpha-2-macroglobulin	3.95E-05	-2.16	Extracellular Matrix Remodeling
VDAC2	P45880	Voltage-dependent anion-selective channel protein 2	3.95E-05	-3.34	Mitochondrial Channel Protein

Molting Outer Blubber Proteome

We identified 2,096 proteins in 184 protein groups in outer blubber tissue in molting elephant seals. Functional annotation of protein groups identified 9 enriched KEGG pathways (adj. $p < 0.05$), which included regulation of glycolysis and gluconeogenesis (n=2), IL-17 signaling (n=2), TNF alpha signaling pathway (n=2), lipid metabolism (n=4), and PI3K/Akt signaling (n=3). Thirteen proteins were upregulated, while eight proteins were downregulated in outer blubber tissue over molting. The magnitude and significance of protein expression changes between samples are presented in Fig. 15b. Manual UniProt database searches were used to infer the functions of DEPs and predict their potential roles in skin regeneration. DEP identifications and functions are listed in Tables 5 and 6. Proteins downregulated over molting in outer blubber included those with known associations with angiogenesis, inflammatory pathways, and lipid

metabolism. Proteins upregulated over molting in the outer blubber tissue included those with known associations with lipid metabolism and mobilization, glycolysis, and cytoskeletal remodeling.

Table 5
Outer blubber Proteins Downregulated by 0.8-Fold or More Over Molting

Gene Symbol	Uniprot Accession	Protein ID	Adjusted P value	Log2 Fold Change	General Functions
EHD1	Q9H4M9	EH domain-containing protein 1	1.42E-04	-0.62	Intracellular Protein Transport
HSP90B1	P14625	Endoplasmin	4.17E-03	-0.92	Heat Shock Chaperone Protein
HBA1	P69905	Hemoglobin subunit alpha	9.29E-03	-2.02	Blood Oxygen Transport
LDHA	P00338	L-lactate dehydrogenase A chain	1.51E-02	-2.44	Glycolytic Enzyme
HSP90AA1	P07900	Heat shock protein HSP 90-alpha	1.82E-04	-3.53	Heat Shock Chaperone Protein
HSPB1	P04792	Heat shock protein beta-1	1.01E-04	-4.44	Heat Shock Chaperone Protein
YWHAB	P31946	14-3-3 protein beta/alpha	6.19E-04	-4.48	Adapter Protein in Signaling Regulation
HBD	P02042	Hemoglobin subunit delta	5.16E-05	-10.45	Blood Oxygen Transport

Table 6
Outer Blubber Proteins Upregulated by 1.2-Fold or Higher Over Molting

Gene Symbol	Uniprot Accession	Protein ID	Adjusted P value	Log2 Fold Change	General Functions
GPD1L	Q8N335	Glycerol-3-phosphate dehydrogenase 1-like protein	1.17E-05	7.787	Carbohydrate Metabolism
SEPTIN7	Q16181	Septin-7	1.93E-03	2.709	Cytoskeletal GTPase
AKR1B1	P15121	Aldo-keto reductase family 1 member B1	6.59E-04	2.941	Glucose Metabolism
ACAA2	P42765	3-ketoacyl-CoA thiolase, mitochondrial	6.39E-03	2.561	Fatty Acid Beta Oxidation
SERPINH1	P50454	Serpin H1	8.93E-04	2.006	Heat Shock Chaperone Protein
SEPTIN2	Q15019	Septin-2	9.95E-03	1.661	Cytoskeletal GTPase Inflammation
GLUL	P15104	Glutamine synthetase	2.44E-03	1.439	Mn-dependent enzyme
AHNAK	Q09666	Neuroblast differentiation-associated protein AHNAK	6.13E-03	1.447	Scaffolding Protein
PPP2R4	Q15257	Serine/threonine-protein phosphatase 2A activator	6.56E-03	1.291	Chaperone Enzyme
APOA1	P02647	Apolipoprotein A-I	1.93E-03	1.237	Lipid Mobilization
PPIA	P62937	Peptidyl-prolyl cis-trans isomerase A	8.63E-03	0.991	Inflammation
EIF5A	P63241	Eukaryotic translation initiation factor 5A-1	6.54E-03	0.725	mRNA-Binding Protein
ALDOA	P04075	Fructose-bisphosphate aldolase A	7.76E-03	0.513	Scaffolding Protein

Discussion

Early Molting

Proteins with higher expression in skin and outer blubber early in the molt haul out, before intensive skin sloughing had begun, included those associated with inflammation, cell

proliferation, cytoskeletal remodeling, angiogenesis, glycolysis, and lipid mobilization in other organisms.

Expression of alpha 2-macroglobulin (A2M), dermatopontin (DPT), and neuroblast differentiation-associated protein (AHNAK) in skin and 14-3-3 protein beta/alpha (YWHAB) in outer blubber early in the molt suggests potential extracellular matrix remodeling in this stage of the molting process. During the proliferative stage of skin regeneration, fibroblasts rapidly proliferate and release growth factors, inducing immune responses, epithelial cell proliferation, collagen deposition, and extracellular matrix remodeling (Dekoninck et al., 2019). The plasma protein A2M, which is expressed in the skin (as well as in liver), stimulates the production of pro-inflammatory cytokines, tumor necrosis factor alpha (TNFα), and interleukin 1 beta (IL1B) (Wedd et al., 1998). A2M has also been shown to bind to and regulate the activity of numerous growth factors and cytokines through inhibition of transforming growth factor (TGFβ) production, implicating A2M as a potential regulator of activity and availability of factors involved in cell proliferation, recruitment, and inflammation (Feigge et al., 1996) (Hiebert et al., 2019) (Kramer et al., 1993). In contrast, DPT, YWHAB, and AHNAK have been shown to increase production of TGFβ and inhibit TNF~~α~~ expression, potentially promoting growth factor signaling and suppressing inflammatory pathways (Kuroda et al., 1999) (Li et al., 2016) (Lee et al., 2014). In previous skin regeneration studies, TGFβ's were implicated as integral components in the wound healing process through induction of epithelial keratinocyte and dermal fibroblast proliferation (Pakyari et al., 2013). Expression of these proteins during early molt suggests potential complex involvement of inflammatory pathways and regulation of the extracellular matrix during the beginning of the molting process, possibly aiding in the skin sloughing phase.

In addition to regulating TGFβ expression, DPT has been implicated as an integral component in maintaining skin elasticity and thickness accumulation, through regulating collagen fibril formation and stability (Brakebusch et al., 2005; Kuroda et al., 1999; Takeda et al., 2002). Additionally, β-tubulin (TUBB), a component of microtubules, is an important regulator of hair bulb melanocyte differentiation in other species (Locher et al., 2015). Studies have also shown reductions in melanocyte proliferation in the absence of β-tubulin (Lehmann et al., 2017). These findings suggest that elevated expression of DPT and TUBB8 in early molt skin may be involved in enhancing extracellular matrix and cytoskeletal remodeling in the epidermal tissue of this organism, which are essential for effective tissue growth and regeneration.

L-lactate dehydrogenase A chain (LDHA) and phosphoglycerate kinase 1 (PGK1), two glycolytic enzymes, were upregulated in early molt in the outer blubber and skin, respectively. LDHA, which is involved in the metabolic conversion of pyruvate to lactate, and PGK1, which catalyzes an ATP-producing step of glycolysis, are both upregulated during anaerobic glycolysis and lactic acid fermentation in other organisms (Rogatzki et al., 2015). Numerous wound healing and cancer studies have reported metabolic reprogramming in fibroblasts isolated from rapidly proliferating cells from oxidative phosphorylation to anaerobic glycolysis followed by lactic acid fermentation for energy metabolism, known and the "Warburg Effect" (Vinaik et al., 2020). Once the cell cycle starts, rapidly proliferating cells rely on glycolysis for ATP generation through glucose uptake, stimulating lactate production and increasing fatty acid synthesis to support the high rate of cellular division. As new skin and hair are developing, rapid proliferation of dermal and epidermal cells is occurring, resulting in a potential shift toward

anaerobic glycolysis for energy metabolism in these cells, possibly contributing to the remarkable speed of skin regeneration in elephant seals.

In addition to its known role in glycolysis, LDHA has also been shown to be essential for angiogenic VEGF production, and its inhibition impairs vascularization and suppresses cell growth (Arik et al., 2019). Additionally, EHD1, an ATP binding protein involved in membrane remodeling and organization, has been shown to induce angiogenesis and vascular endothelial cell proliferation in epithelial tissues through interactions with IGF-1 (Wang et al., 2019). In addition to inflammation and extracellular matrix remodeling, development of new blood vessels often occurs during the proliferative stage of wound healing as well. Vascularization is an essential component of tissue regeneration, as it provides the developing tissue with oxygenated and nutrient-rich blood (Tonneson et al., 2000). Accordingly, two hemoglobin subunits (HBB and HBA1) were expressed highly during early molt in outer blubber, likely as a consequence of increased blood vessel density and erythrocyte recruitment during this time.

Endoplasmin (HSP90B1), heat shock protein HSP 90-alpha (HSP90AA1), heat shock protein beta-1 (HSPB1), L-lactate dehydrogenase A chain (LDHA), and EH domain-containing protein 1 (EHD1), expressed highly during early molt in outer blubber, have been associated with regulation of growth factor secretion, extracellular matrix development, and angiogenesis in other organisms. The heat shock proteins identified in this study have been linked to increased blood vessel formation and cellular proliferation through the VEGF signaling pathway (Takahashi et al., 2003) (Lee et al., 2012). High expression of heat shock proteins in the outer blubber during molting may facilitate the synthesis and secretion of growth factors and ECM proteins that support the developing skin, as well as enable its vascularization.

These findings suggest that molting, in the early stages, may involve increased inflammatory and angiogenic pathways in the blubber tissue as the new dermal layers develop and an upregulation of glycolysis related proteins may support the high metabolic requirements of rapidly proliferating cells within the hypodermis. However, we did not detect upregulation of proteases or pro-apoptotic proteins in early molt as we had hypothesized, since degradation of extracellular components and cell-matrix anchors, such as desmosomes are necessary for desquamation (Has et al., 2018). Consequently, additional sampling throughout the molt is needed to more accurately identify the mechanisms triggering the onset of skin cell death and sloughing.

Late Molting

Protein upregulated in skin and outer blubber during the late molt haul out, when pelage shedding has been completed and active hair growth is ongoing, included those associated with protein synthesis, extracellular matrix synthesis and remodeling, and lipid mobilization.

Tissue regeneration and hair growth involves intensive protein synthesis (Dekoninck et al., 2019), which was supported by the upregulation of five ribosomal proteins – RPL17, RPL10, RPL10A, RPL8, and RPLP0P6 – over molting in the skin. Ribosomal proteins have been linked to numerous physiological functions including cell growth, immune and inflammatory pathway regulation, and apoptosis, which are all likely involved in molting (Zhou et al., 2015). Type I alpha 2 collagen (COLIA2), and vimentin (VIM) were upregulated in skin and serpin H1 (SERPINH1/HSP47), glutamine synthetase (GLUL), and neuroblast differentiation-associated protein (AHNAK) were upregulated in outer blubber during late molt, suggesting an increase in collagen synthesis and organization during the time of rapid skin growth and thickening. COLIA2, the fibrillar collagen found in connective tissue, supports tissue growth and repair

through intracellular assembly of procollagen molecules and extracellular assembly of collagen fibrils (Liu et al., 2016). SERPINH1, a collagen chaperone protein, is expressed in the endoplasmic reticulum and synthesizes both type I and type II collagen (Razzaque et al., 2002). VIM, a major cytoskeletal component of mesenchymal cells, has emerged as a signaling integrator in tissue regeneration and wound healing studies (Cheng et al., 2016). GLUL, an enzyme that catalyzes the conversion of glutamate to glutamine in metabolic pathways, has been shown to play a key role in regulation of skin fibroblast proliferation and is upregulated in response to elevated corticosteroids (Vermeulen et al., 2008), which increase over molting in seals (see Chapter 3). AHNAK, as previously described in early molt skin, VIM, SERPINH1, and GLUL have all been shown to increase TGFβ signaling, thereby promoting fibroblast proliferation and keratinocyte differentiation and limiting inflammation (Wang et al., 2017) (Razzaque et al., 2002) (Vermeulen et al., 2008). These findings suggest that COLIA2, SERPINH1, VIM, AHNAK, and GLUL may be involved in stimulating proliferation of epithelial cells, inhibiting inflammation during active tissue growth, and promoting collagen deposition and remodeling during late molting. This supports that late molting in seals is similar to the maturation phase of tissue regeneration, which is characterized by extensive ECM remodeling and reduction in inflammation and angiogenesis.

Proteins upregulated during late molt also included PDZ and LIM domain protein 1 (PDLIM1), poly(rC)-binding protein 1 (PCBP1), and cysteine and glycine-rich protein 1 (CSRP1) in the skin. Overexpression of PDLIM1, a cytoskeletal protein involved in fibroblast assembly, has been shown to inhibit metastasis during epithelial–mesenchymal transition through the hippo signaling pathway (Chen et al., 2016) (Huang et al., 2020). PCBP1, a nucleic acid binding protein involved in regulation of mRNA transcription, has been shown to inhibit

metastasis and tumorigenesis through modulation of Akt signaling (Lee et al., 2014). CSRP1, an actin binding protein, has been shown to inhibit cytoskeletal growth and suppress keratinocytes proliferation in the presence of excess UV radiation, to which seals are exposed to when hauled out on land (Latonin et al., 2010). Taken together, these findings suggest that upregulation of these proteins may serve to limit cellular proliferation and growth at the end of the molting process.

Upregulation of proteins involved in lipid mobilization and transport and carbohydrate metabolism over molting are to be expected in this fasting-adapted organism. Glycerol-3-phosphate dehydrogenase 1-like protein (GPD1L), 3-ketoacyl-CoA thiolase (ACAA2), apolipoprotein A-1 (APOA1), aldolase A (ALDOA), and aldo-keto reductase (AKR1B1), expressed in the outer blubber, and cytochrome P450 (CYP1A1) and aldo-keto reductase (AKR1B1) expressed in the skin, are associated with carbohydrate and lipid metabolism in other organisms and were upregulated in the late molt samples. GPD1L regulates carbohydrate and lipid metabolism by catalyzing the conversion of DHAP and NADH to G3P and NAD+ (Joshua et al., 2019). Overexpression of GPD1L has been positively correlated with insulin sensitivity and hypoxia-induction factor (HIF) degradation in obesity weight loss-related studies in humans (He et al., 2017), suggesting that this protein may potentially be involved in regulating fasting metabolism in a hypoxia-adapted, insulin-resistant mammal with large lipid stores. Upregulation of ACAA2 and CYP1A1, two enzymes involved in fatty acid beta-oxidation (Yang et al., 2018), is consistent with the high rates of lipid oxidation reported in fasting northern elephant seals (Crocker et al., 2014). ALDOA, a glycolytic enzyme that catalyzes the conversion of fructose-1,6-bisphosphate to G3P and DHAP (Kuehne et al., 2017), is also upregulated during fasting in other organisms, and was recently shown to induce apoptosis in tumor tissues (Ma et al., 2018).

This suggests that upregulation of ALDOA during late molt may be involved in both regulating fasting metabolism and inhibiting excessive cell proliferation at the completion of molting. AKR1B1, an enzyme involved in the catalytic reduction of aldehydes and ketones, has been shown to be involved in oxidative stress responses, cell signal transduction, cell proliferation, and steroid synthesis (Khayami et al., 2020). APOA1 functions in cholesterol transport to steroidogenic tissues for corticosteroid hormone synthesis (Fournier et al., 1999). The upregulation of AKR1B1 and APOA1 may play a role in supporting the production of large amounts of corticosteroids over the molting period (see Chapter 4), potentially locally in outer blubber as well as in the adrenal gland.

Skin molting during the late stages results in rapidly regenerated hair and epithelial cells and, as expected, results in an increase in abundance of proteins associated with protein synthesis and extracellular matrix remodeling. Since these seals undergo this molting period while fasting, an upregulation of proteins associated with lipid mobilization and metabolism over the molt are also to be expected. Tissue regeneration in the maturation or late stage involves intensive collagen deposition and protein synthesis in the developing tissues, which was supported in this study by the upregulation of ribosomal, extracellular matrix, and fibroblast-stimulating proteins during late molt. However, cell proliferation in newly formed skin may be limited by upregulation of tumor suppressor proteins that act in a counter-regulatory manner, restricting excess epithelial growth at the end of molting.

CHAPTER 5: GENE EXPRESSION CHANGES IN RESPONSE TO CATASTROPHIC MOLTING

Introduction

Phenotypic expression is regulated by numerous mechanisms within cellular division and replication including, but not limited to, transcription of DNA into RNA and translation of mRNA to amino acid chains, resulting in the formation of proteins (Vogel et al., 2012). Although changes in protein abundance during catastrophic molting were previously described in Chapter 4, whether these changes were the result of regulation at the transcriptional or post-transcriptional levels have not been examined. Implementation of proteomics, when coupled with gene expression analyses, can be used to identify potential mechanisms driving changes in protein abundance that underlie phenotypic expression of molting.

I used reverse transcription and real-time polymerase chain reaction (RT-qPCR) to compare expression of mRNA transcripts encoding proteins that were differentially expressed during molting in the same skin and outer blubber samples described in Chapter 4. We hypothesized the metabolic enzymes GLUL, GPD1L, and ACAA2, which were upregulated over molting at the protein level, would also be upregulated in blubber at the transcript level, whereas YWHAB would be downregulated over molting. Additionally, based on their expression at the protein level, expression of mRNA transcripts encoding CSRP1 and VIM are expected to be higher in the late molt skin samples, whereas A2M and VDAC2 are expected to be higher in the early molt skin samples.

Methods

Sample Collection

Skin and outer blubber samples were collected from adult female northern elephant seals (n = 6) at Año Nuevo State Reserve (San Mateo County, CA) during the summer 2020 molting period by methods previously described in Chapter 2 and Chapter 4.

Sample Preparation

RNA isolation and quantification. Skin and blubber samples were homogenized by bead beating in Trizol (Ambion, USA; ~50mg tissue per 1.0 mL) or Qiazol (Qiagen, USA; ~100mg tissue per 1.0 mL), respectively, using 2.0-mL tubes pre-filled with 2.4-mm metal beads (Fisher Scientific, USA) using the Bullet Blender Storm 24 (Next Advance, USA; Speed 12, two 2-minute cycles). RNA was extracted using chloroform phase extraction according to manufacturers' protocols (12,000g x 15 min at 4°C). RNA was precipitated from the blubber and skin samples using 70% ethanol or 100% isopropanol, respectively. Blubber and skin RNA was purified using the RNeasy Lipid Mini Kit (Qiagen, USA) and RNeasy Mini Kit (Qiagen, USA), respectively, which both involved a 15-min on-column DNase 1 (Qiagen, USA) digest. RNA quality was determined using the Qubit 3.0 Fluorometer Broad-Range RNA Assay (Life Technologies, USA). RNA quality was assessed using the Total RNA Pico Kit on the 2100 Bioanalyzer (Agilent Technologies). Average RNA Integrity Number (RIN) for the blubber samples was 7.15 and 9.12 for the skin samples.

Reverse transcription (RT). 500ng of RNA from each sample was reverse transcribed to complementary DNA (cDNA) using SuperScript IV VILO Master Mix with ezDNase digestion, following the manufacturer' protocol (Thermo Fisher, USA). Resulting cDNA samples were diluted 1:10 with water for qPCR.

Primer design. Genes of interest encoding differentially expressed proteins discussed in Chapter 3 were selected for transcript expression analysis by qPCR (Table 7). Four genes were selected from the outer blubber molting proteome, three of which were upregulated over molting (GPD1L, ACAA2, GLUL) and one of which was downregulated over molting (YWHAB). Five genes were selected from the skin molting proteome, three of which were upregulated over molting (VIM, CSRP1, CYP1A1) and two were downregulated over molting (A2M, VDAC2). Primers were designed to target a portion of the transcript that encoded a conserved sequence of the protein using transcriptomes from elephant seal blubber (Deyarmin et al., 2019) and skin-derived fibroblasts (Khudyakov et al., unpublished). Primers were selected to have a product size between 95-110 base pairs and have melting temperatures (Tm) of 62°C. YWHAZ and NONO were evaluated as reference genes, due to previous use in gene expression analyses of elephant seal blubber tissue (Khudyakov et al., 2017).

Table 7
List of Candidate Genes for Evaluating Gene Expression Over Molting

Transcript IDs	Tissue	Gene Homolog	Protein Name	Forward Primer Sequence	Reverse Primer Sequence
TRINITY_DN173427_c8_g4_i1 TRINITY_DN592286_c3_g1_i7 TRINITY_DN592286_c3_g1_i16 TRINITY_DN592286_c3_g1_i41	Skin	A2M	Alpha-2-macroglobulin	GAGGCCAAGATCCAAGAAGAA	GGGTCCACTTTCACGAATGA
TRINITY_DN592650_c1_g1_i6 TRINITY_DN592650_c1_g1_i9 TRINITY_DN592650_c1_g1_i19	Skin	CSRP1	Cysteine and glycine-rich protein 1	GTGTGCCAGAAGACGGTTTA	GGTGCTGTCCAGATTCTTCTT
TRINITY_DN175447_c5_g1_i5 TRINITY_DN175447_c5_g1_i7	Skin	VDAC2	Voltage-dependent anion-selective channel protein 2	CCCTTGAGTTGGAGGCTTAAT	GGGTCCACTTTCACGAATGA
TRINITY_DN593268_c10_g1_i8 TRINITY_DN593268_c10_g1_i9	Skin	VIM	Vimentin	CCATCAACACCGAGTTCAAGA	CGCACCTTGTCGATGTAGTT
TRINITY_DN589746_c3_g2_i8 TRINITY_DN589746_c3_g2_i16	Outer Blubber	ACAA2	3-ketoacyl-CoA thiolase, mitochondrial	GATGGTGCTGGAGCTGTTAT	ATCACATCCGGACACAAAGTAG
TRINITY_DN593465_c0_g1_i9 TRINITY_DN593465_c0_g1_i13	Outer Blubber	GLUL	Glutamine synthetase	CAACGAAACTGGCGATGAAC	TGGAGGCAAGATGGAGAATTAG
TRINITY_DN581200_c4_g2_i9 TRINITY_DN581200_c4_g2_i11	Outer Blubber	GPD1L	Glycerol-3-phosphate dehydrogenase 1-like protein	CAGCAAGTTCCAAACAGCTTAG	TCAGGTCACCATAGCCTAGAA
TRINITY_DN588358_c1_g2_i3 TRINITY_DN588358_c1_g2_i7 TRINITY_DN588358_c1_g2_i8	Outer Blubber	YWHAB	14-3-3 protein beta/alpha	CCAATGCTACACAACCAGAAAG	CAGATGCCACCTCAGAAAGATA

Note. Primer sequences are listed in the 5’ to 3’ direction.

Real-time PCR (qPCR). Primers were used at 400 nM concentration in a 20uL reaction with Power Up SYBR Green Master Mix (Thermo Fisher, USA). Each reaction was run in triplicate on a QuantStudio 5 Real-Time PCR System instrument (Thermo Fisher, USA) using the following program: 2 min at 50°C, 2 min at 95°C, followed by 40 cycles of 15sec at 95°C, and 60sec at 60°C. Gene expression was determined by the cycle threshold (Ct) of the qPCR cycle in which fluorescent amplicons were first detected.

Expression analyses. Cts for each gene of interest were normalized to the Cts of the reference gene, NONO, to obtain delta Ct values [dCt = Ct of reference gene - Ct of interest] (Livak et al., 2001). Stability of reference gene expression across samples was evaluated using RefFinder (Xie et al., 2012). All replicate SDs were < 0.105 Ct, as recommended by MIQE Guidelines (Bustin et al., 2009). No-template and no-reverse transcriptase controls were included in each run and showed no amplification. Melt curve analysis was used to confirm primer specificity by the presence of a single product. Differential expression analysis was run in R v4.2.0 (R Core Team, 2016; R Core Team, 2019) using an unpaired t-test.

Results

Eight target genes, previously identified to be differentially expressed during molting at the protein level in Chapter 3, were evaluated for similar expression changes at the transcript level. The four outer blubber genes, ACAA2, GLUL, GPD1L, and YWHAB, did not display significant differences in transcript expression between molting classes (ACAA2: p=0.93, GLUL: 0.19, GPD1L: 0.35, YWHAB: 0.69,). Additionally, transcripts encoding the four skin proteins (A2M: p=0.39, CSRP1: 0.17, VDAC2: 0.63, and VIM: 0.17) also did not display significant differences between molting stages. Despite the lack of statistically significant differences in transcript expression between early and late molting, three genes, GLUL, GPD1L,

and VIM, did display similar trends in transcript expression to protein expression changes described in Chapter 3, specifically increase in abundance during late molting.

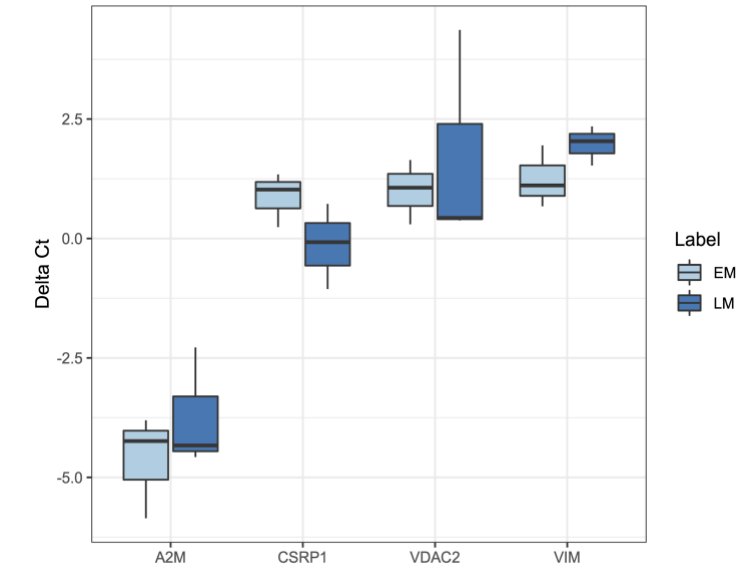

A

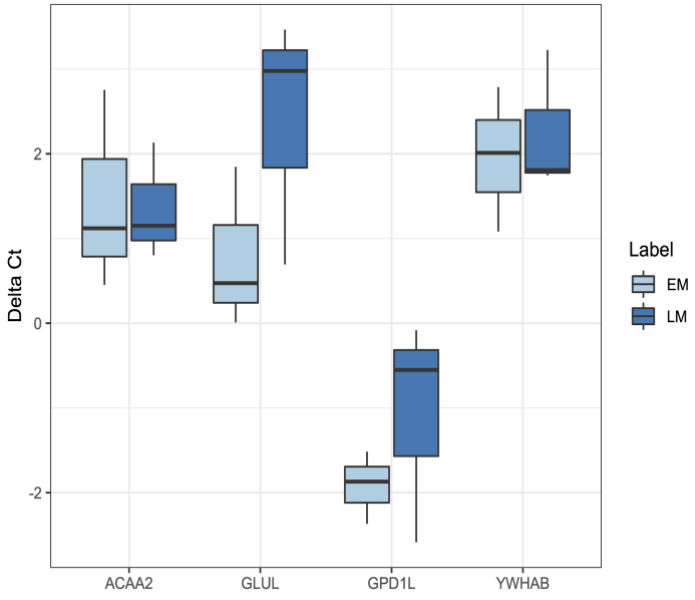

B

Figure 16. Box and whisker plot depicting normalized transcript expression levels (delta CT) of A) skin and B) outer blubber gene expression. No superscripts present as the genes did not display statistically significant differences between molting stages.

Discussion

The lack of significant differences in gene expression over molting was not surprising due to the limited sample size, individual variability between unmatched study subjects, relative instability of RNA compared to proteins, and the temporal mismatch between gene and protein expression changes within the same cells. Several studies have shown that analyzing transcriptome and proteome data collected from the same samples simultaneously often do not agree (Liu et al., 2016; Vogel et al., 2012, Deyarmin et al., 2019). Nevertheless, these data provide the first insights into molecular responses to catastrophic molting and tissue regeneration in a marine mammal and lay the foundation for future studies aimed at further evaluation of identified biomarkers. Expression of three genes, GLUL, GPD1L, and VIM, which encode the metabolic enzymes glutamine synthetase and glycerol-3-phosphate dehydrogenase 1-like protein and the cytoskeletal protein vimentin, though not significantly different between molting classes, did display similar trends when compared to the proteomic data described in Chapter 4. Thus, these genes may be promising candidates for further research on natural molting processes in mammals and tissue regeneration in humans.

CHAPTER 6: SYNTHESIS AND FUTURE DIRECTIONS

Skin and hair regeneration is a complex process involving a fine balance of molecular, cellular, and endocrine mechanisms. This study provides the first skin proteome of northern elephant seals and the first exploration of cellular mechanisms regulating catastrophic molting in mammals. Using histological, metabolic, and molecular evaluation of serum and skin and outer blubber tissues obtained from a wild marine mammal, the northern elephant seal, that tissue regeneration may be influenced by corticosteroids and thyroid hormones and involves regulation of extracellular matrix remodeling and inflammatory, angiogenic, and glycolytic pathways (Fig. 17).

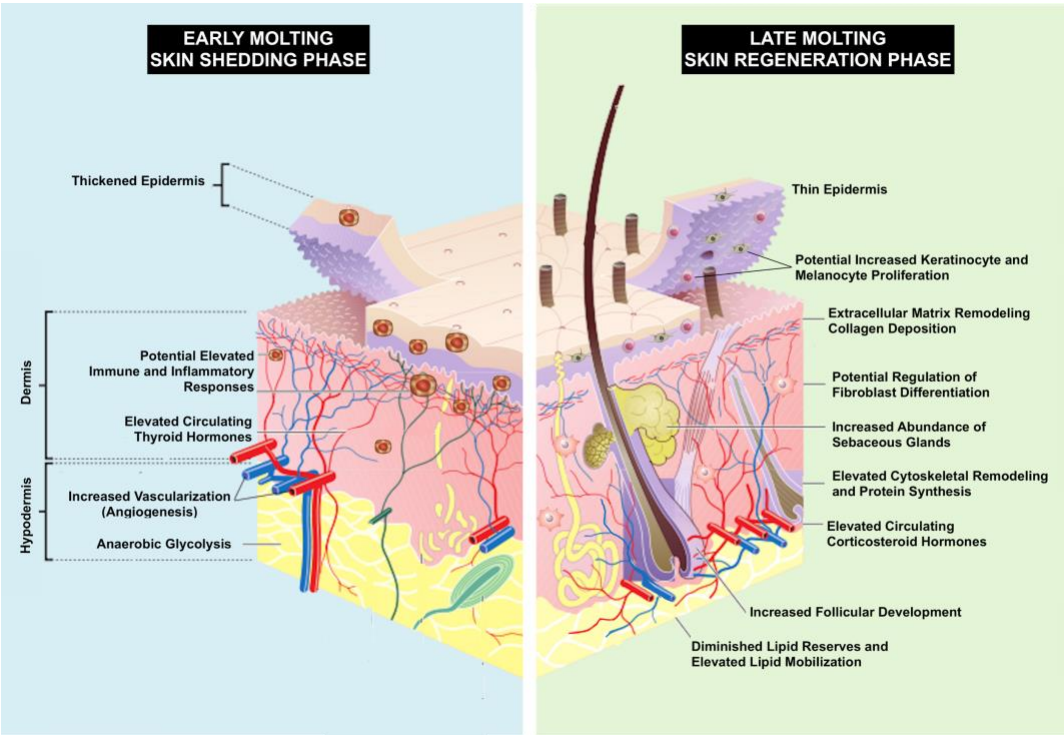

Figure 17. Synthesis of potential functions present during early and late molting. Figure adapted from "Skin_layers.Png." https://Commons.wikimedia.org

Early molting, similar to the proliferative stage of tissue regeneration in other studied species, involves shedding of epidermal tissue and rapid loss of aging hairs, potentially induced by changes in corticosteroid and thyroid hormone levels and apoptotic signals from the dermis and/or hypodermis. Higher levels of thyroid hormones in early molt compared with upregulation of several proteins that are known thyroid hormone receptor targets: heat shock proteins, hemoglobin subunits, LDHA, and YWHAB (Chen et al., 2012; Wallen et al., 2012; Zexin et al., 2020). Additionally, upregulation of proteins involved in TGFB and TNFA signaling (A2M, DPT, AHNAK, and YWHAB) suggests involvement of inflammation and extracellular matrix degradation and remodeling during this phase. Interestingly, early molting in seals may also involve a tissue-specific switch to anaerobic glycolysis followed by lactic acid fermentation for energy metabolism to keep up with the high rate of cellular proliferation, a common phenomenon observed during tumorigenesis. Finally, potentially increased vascularization in the underlying blubber tissue layers, which was suggested by elevated expression of heat shock proteins (HSP90B1, HSP90AA1, HSPB1), LDHA, and EHD1 during early molt, may provide nutritional and blood oxygen supply to the new developing hypodermis.

Tissue regeneration, in the late stages of molting, involves a tightly controlled regulation of collagen synthesis and organization and follicular and sebaceous gland growth, consistent with findings in other pinniped and mammalian species. The late molt histology images showed hair follicles in a stage of growth and proliferation, which was supported by upregulation of proteins involved in protein synthesis and extracellular matrix remodeling (COL1A2, VIM, GLUL, AHNAK, SERPINH1, and five ribosomal proteins). Upregulation of corticosteroids in late molting may play a role in regulating lipid mobilization during fasting and controlling cellular proliferation in the developing epidermis through expression of known corticosteroid-

regulating proteins (AKR1B1, APOA1, and ALDOA). Additionally, the known pro-apoptotic functions of corticosteroids coupled with upregulation of proteins associated with inhibition of cell proliferation (PDLIM1, PCBP1, CSRP1), suggests restricted proliferation at the end of molting to avoid tumorigenesis.

Although some mechanisms involved in catastrophic molting were identified, there were limitations to this study, specifically small sampling size, cross-sectional sampling design, and individual variability that reduced sensitivity for detecting differences in gene and protein expression between molting stages. The comparison of epidermal thickness between early and late molting not only documents skin sloughing has taken place, but also suggests that additional epidermal thickening and development occurs after the seals leave the rookery and return to foraging. Additionally, we did not detect upregulation of proteases, pro-apoptotic factors, or other proteins involved in desquation (Has et al., 2018) in our proteome, suggesting that the mechanisms enabling skin sloughing may be initiated at sea, before the molt haul out has begun. Therefore, future studies should conduct additional, longitudinal sampling throughout the molting haul out, as well as during the preceding and following breeding haul outs to document the full catastrophic molting profile. In addition, sampling a larger number of animals, including other age classes such as adult females and males, will increase statistical power for transcriptome and proteome analysis and may provide more insights into the common (rather than age- or sex-specific) molecular mechanisms enabling molting in this species. Despite these limitations, the shotgun proteomics approach used in this study enabled the identification and functional annotation of hundreds of proteins in this non-model organism, and the discovery of potential mechanisms of rapid skin regeneration in wild mammals. Further investigative studies,

targeting mechanisms identified in this study, may be able to be applied towards therapeutic approaches in rapid skin regeneration for other mammal species.

REFERENCES

Abdallah F, et al. *Skin Immune Landscape: Inside and Outside the Organism.* Mediators Inflamm. 2017;2017:5095293.

Andreasson U, et al. *A Practical Guide to Immunoassay Method Validation*. Front Neurol, 2015 Aug 19;6:179.

Andrews R, et al. *Platelet physiology and thrombosis.* Thromb Res, 2004;114(5-6):447-53.

Antonini D, et al. *An intimate relationship between thyroid hormone and skin: regulation of gene expression*. Front. Endocrinol, 2013:4:104.

Arik, et al. *The role of glycolysis and mitochondrial respiration in the formation and functioning of endothelial tip cells during angiogenesis*. Sci Rep, 2019. 9. 1-14. 10.1038/s41598-019-48676-2.

Ashwell-Erickson S, et al. *Metabolic and hormonal correlates of molting and regeneration of pelage in Alaskan harbor and spotted seals (Phoca vitulina and Phoca largha).* Canadian Journal of Zoology. 64(5): 1086-1094.

Aurora A, et al. *Immune modulation of stem cells and regeneration*. Cell Stem Cell, 2014 Jul 3;15(1):14-25.

Beltran R, et al. *Convergence of biannual moulting strategies across birds and mammals.* Biological sciences, 2018: 20180318.

Boix J, et al. *Primary aldosteronism patients show skin alterations and abnormal activation of glucocorticoid receptor in keratinocytes.* Sci Rep, 2017.

Brakebusch C, et al. *Beta 1 integrin function in vivo: adhesion, migration and more.* Cancer Metastasis Rev, 2005 Sep;24(3):403-11.

Bustin S, et al. *The MIQE guidelines: minimum information for publication of quantitative real-time PCR experiments*. Clin Chem. 2009 Apr;55(4):611-22.

Champagne C, et al. *Adrenal sensitivity to stress is maintained despite variation in baseline glucocorticoids in moulting seals.* Conservation Physiology, 2015.

Chen E, et al. *Enrichr: interactive and collaborative HTML5 gene list enrichment analysis tool*. BMC Bioinformatics, 2013 Apr 15;14:128.

Chen H, et al. *PDLIM1 Stabilizes the E-Cadherin/β-Catenin Complex to Prevent Epithelial-Mesenchymal Transition and Metastatic Potential of Colorectal Cancer Cells*. Cancer Res, 2016 Mar 1;76(5):1122-34.

Chen M, et al. *Promotion of the induction of cell pluripotency through metabolic remodeling by thyroid hormone triiodothyronine-activated PI3K/AKT signal pathway.* Biomaterials, 2012: 5514-23 .

Chen Y, et al. *Brain-skin connection: stress, inflammation and skin aging.* Inflammation & allergy drug targets vol. 13,3, 2014: 177-90.

Cheng F, et al. *Vimentin coordinates fibroblast proliferation and keratinocyte differentiation in wound healing via TGF-β-Slug signaling*. Proc Natl Acad Sci USA, 2016 Jul 26;113(30):E4320-7.

Chuong C, et al. *What is the 'true' function of skin?* Exp Dermatol, 2002 Apr;11(2):159-87.

Crespi E, et al. *Life history and the ecology of stress: how do glucocorticoid hormones influence life-history variation in animals.* Funct Ecol, 2013 27: 93-106.

Crocker D, et al. *Adiposity and fat metabolism in lactating and fasting northern elephant seals.* Advances in nutrition (Bethesda, Md.), 2014.

Cui X, et al. *HIF1/2α mediates hypoxia-induced LDHA expression in human pancreatic cancer cells.* Oncotarget, 2017: 24840-24852.

Dekoninck S, et al. *Stem cell dynamics, migration and plasticity during wound healing.* Nat Cell Biol 21, 18–24, 2019.

Deyarmin JS, et al. *Blubber transcriptome responses to repeated ACTH administration in a marine mammal*. Sci Rep, 2019 Feb 25;9(1):2718.

Eyerich S, et al. *Cutaneous Barriers and Skin Immunity: Differentiating A Connected Network.* Trends Immunol, 2018 Apr;39(4):315-327.

Feige JJ, et al. *Alpha 2-macroglobulin: a binding protein for transforming growth factor-beta and various cytokines.* Horm Res, 1996;45(3-5):227-32.

Finch C, et al. *Hormones and the physiological architecture of life history evolution.* Q Rev Biol. 1995 Mar;70(1):1-52.

Fischer A, et al. *Cutting sections of paraffin-embedded tissues.* CSH Protocols, 2008.

Fischer A, et al. *Hematoxylin and eosin staining of tissue and cell sections.* CSH Protocols, 2008.

Fischer A, et al. *Paraffin embedding tissue samples for sectioning.* CSH Protocols, 2008.

Fournier N, et al. *Fractional efflux and net change in cellular cholesterol content mediated by sera from mice expressing both human apolipoprotein AI and human lecithin:cholesterol acyltransferase genes*. Atherosclerosis, 1999 Dec;147(2):227-35.

Fröbel J, et al. *Platelet proteome analysis reveals integrin-dependent aggregation defects in patients with myelodysplastic syndromes.* Molecular & cellular proteomics, 2013: 1272-80.

Grachtchouk M, et al. *Basal cell carcinomas in mice arise from hair follicle stem cells and multiple epithelial progenitor populations.* J Clin Invest, 2011:121(5):1768–81.

Gruber R, et al. *Sebaceous gland, hair shaft, and epidermal barrier abnormalities in keratosis pilaris with and without filaggrin deficiency.* Am J Pathol, 2015 Apr;185(4):1012-21.

Gruver-Yates A, et al. *Tissue-specific actions of glucocorticoids on apoptosis: a double-edged sword*. Cells. 2013 Mar 26;2(2):202-23.

Has C. *Peeling Skin Disorders: A Paradigm for Skin Desquamation*. J Invest Dermatol, 2018 Aug;138(8):1689-1691

He H, et al. *A Systems Genetics Approach Identified GPD1L and its Molecular Mechanism for Obesity in Human Adipose Tissue.* Sci Rep, 2017.

Hiebert P, et al. *Regulation of Wound Healing by the NRF2 Transcription Factor-More Than Cytoprotection.* Int J Mol Sci, 2019 Aug 8;20(16):3856.

Huang Z, et al. *PDLIM1 Inhibits Tumor Metastasis Through Activating Hippo Signaling in Hepatocellular Carcinoma.* Hepatology, 2020 May;71(5):1643-1659.

Jelincic JA, et al. *Variation in adrenal and thyroid hormones with life-history stage in juvenile northern elephant seals (Mirounga angustirostris).* Gen Comp Endocrinol, 2017 Oct 1;252:111-118.

Kenessey A, et al. *Thyroid hormone stimulates protein synthesis in the cardiomyocyte by activating the Akt-mTOR and p70S6K pathways.* J Biol Chem. 2006 Jul 28;281(30):20666-72.

Khayami R, et al. *Role of aldo-keto reductase family 1 member B1 (AKR1B1) in the cancer process and its therapeutic potential.* Journal of cellular and molecular medicine, 2020: 8890-8902.

Khudyakov J, et al. *Blubber transcriptome response to acute stress axis activation involves transient changes in adipogenesis and lipolysis in a fasting-adapted marine mammal*. Sci Rep, 2017 Feb 10;7:42110.

Khudyakov J, et al. *Muscle transcriptome response to ACTH administration in a free-ranging marine mammal.* Physiol Genomics, 2015 Aug;47(8):318-30.

Khudyakov J, et al. *Transcriptome analysis of northern elephant seal (Mirounga angustirostris) muscle tissue provides a novel molecular resource and physiological insights.* BMC Genomics, 2015.

Kolde R, et al. 2019. *pheatmap: Pretty Heatmaps*. Available online at: https://CRAN.R-project.org/package=pheatmap (accessed November 29, 2020).

Kozyraki R, et al. *The intrinsic factor-vitamin B12 receptor, cubilin, is a high-affinity apolipoprotein A-I receptor facilitating endocytosis of high-density lipoprotein*. Nat Med, 1999 Jun;5(6):656-61.

Kramer MD, et al. *The autoimmune blistering skin disease bullous pemphigoid. The presence of plasmin/alpha 2-antiplasmin complexes in skin blister fluid indicates plasmin generation in lesional skin*. J Clin Invest, 1993 Aug;92(2):978-83.

Kuehne A, et al. *An integrative metabolomics and transcriptomics study to identify metabolic alterations in aged skin of humans in vivo*. BMC Genomics, 2017.

Kuleshov M, et al. *Enrichr: a comprehensive gene set enrichment analysis web server 2016 update.* Nucleic Acids Res, 2016 Jul 8;44(W1):W90-7.

Kuroda K, et al. *Dermatopontin expression is decreased in hypertrophic scar and systemic sclerosis skin fibroblasts and is regulated by transforming growth factor-beta1, interleukin-4, and matrix collagen*. J Invest Dermatol, 1999 May;112(5):706-10.

Lai-Cheong J, et al. *Structure and function of skin, hair and nails*. Medicine, Volume 37, Issue 5, 2009.

Latonen L, et al. *Ultraviolet B radiation regulates cysteine-rich protein 1 in human keratinocytes.* Photodermatology, Photoimmunology & Photomedicine, 2010: 26: 70-77.

Le Boeuf B, et al. *Foraging Ecology of Northern Elephant Seals*. Ecological Monographs, 2000. 70: 353-382.

Le Boeuf BJ, et al. *Elephant Seals: Population Ecology, Behavior, and Physiology*. University of California Press, 1994.

Lee I, et al. *Ahnak functions as a tumor suppressor via modulation of TGFβ/Smad signaling pathway*. Oncogene, 2014. 33, 4675–4684

Lee YJ, et al. *Soluble HSPB1 regulates VEGF-mediated angiogenesis through their direct interaction.* Angiogenesis. 2012 Jun;15(2):229-42.

Lehmann S, et al. *Tubulin Beta-3 Chain as a New Candidate Protein Biomarker of Human Skin Aging: A Preliminary Study*. Oxid Med Cell Longev, 2017.5140360. doi: 10.1155/2017/5140360. Epub 2017 May 23. PMID: 28626498; PMCID: PMC5463169.

Li P, et al. *Identification of NF-κB inhibitors following Shenfu injection and bioactivity-integrated UPLC/Q-TOF-MS and screening for related anti-inflammatory targets in vitro and in silico*. J Ethnopharmacol, 2016 Dec 24;194:658-667.

Ling J et al. *Pelage and Molting in Wild Mammals with Special Reference to Aquatic Forms*. JSTOR. The Quarterly Review of Biology, vol. 45, no. 1, 1970, pp. 16–54.

Ling J, et al. *A histological study of the skin, hair follicles and moult of the hooded seal (Cystophora cristata*. Polar Research, 2018. 37.1419906. 10.1080/17518369.2017. 1419906.

Liu J, et al. *Downregulation of let-7b promotes COL1A1 and COL1A2 expression in dermis and skin fibroblasts during heat wound repair*. Mol Med Rep, 2016 Mar;13(3):2683-8.

Liu S, et al. *Expression of integrin beta1 by fibroblasts is required for tissue repair in vivo.* J Cell Sci, 2010 Nov 1;123(Pt 21):3674-82.

Liu Y, et al. *On the Dependency of Cellular Protein Levels on mRNA Abundance*. Cell. 2016 Apr 21;165(3):535-50.

Livak K, et al. *Analysis of relative gene expression data using real-time quantitative PCR and the 2(-Delta Delta C(T)) Method*. Methods, 2001 Dec;25(4):402-8.

Locher H et al. *Hair follicle bulge cultures yield class III β-tubulin-positive melanoglial cells.* Histochemistry and cell biology, 2015. 87-91.

Moeller L, et al. *Cytosolic action of thyroid hormone leads to induction of hypoxia-inducible factor-1alpha and glycolytic genes*. Mol Endocrinol, 2005:19(12):2955–63.

Niemann C, et al. *Development and homeostasis of the sebaceous gland.* Seminars in cell & developmental biology, 2012: 928-36.

Oliver S, et al. *Model organism databases: essential resources that need the support of both funders and users.* BMC Biol, 2016. 14: p. 49.

Pakyari M, et al. *Critical Role of Transforming Growth Factor Beta in Different Phases of Wound Healing.* Advances in wound care, 2013: 215-224.

Paus R, et al. *Chronobiology of the hair follicle: hunting the hair cycle clock*. J Investig Dermatol Symp Proc, 1999 Dec;4(3):338-45.

Plötz, M et al. *Disruption of the VDAC2-Bak interaction by Bcl-x(S) mediates efficient induction of apoptosis in melanoma cells.* Cell death and differentiation vol. 19,12 (2012): 1928-38.

Razzaque M, et al. *Collagens, collagen-binding heat shock protein 47 and transforming growth factor-beta 1 are induced in cicatricial pemphigoid: possible role(s) in dermal fibrosis.* Cytokine, 2002 Mar 21;17(6):311-6.

Ritchie M, et al. *Limma powers differential expression analyses for RNA-sequencing and microarray studies*. Nucleic Acids Res, 2015 Apr 20;43(7):e47.

Rogatzki M, et al. *Lactate is always the end product of glycolysis.* Frontiers in neuroscience vol. 9 22. 27 Feb. 2015.

Rojas-Pirela M, et al. *Phosphoglycerate kinase: structural aspects and functions, with special emphasis on the enzyme from Kinetoplastea.* Open biology, 2020: 200302.

Russell J, et al. *Non-model model organisms*. BMC Biol, 2017. 15(1): p. 55.

Sheppard H, et al. *AHNAK is downregulated in melanoma, predicts poor outcome, and may be required for the expression of functional cadherin-1*. Melanoma Res, 2016 Apr;26(2):108-16.

Shi VY, et al. *Role of sebaceous glands in inflammatory dermatoses*. J Am Acad Dermatol, 2015 Nov;73(5):856-63.

Shijun L, et al. *Function and characterization of the promoter region of perilipin 1 (PLIN1): Roles of E2F1, PLAG1, C/EBPβ, and SMAD3 in bovine adipocytes.* Genomics, 2020 May;112(3):2400-2409.

"Skin_layers.Png." Https://Commons.wikimedia.org, 11 Mar. 2011.

Slenter D, et al. *WikiPathways: a multifaceted pathway database bridging metabolomics to other omics research.* Nucleic Acids Res, 2018 Jan 4;46(D1):D661-D667.

Sohn M, et al. *Ahnak promotes tumor metastasis through transforming growth factor-β-mediated epithelial-mesenchymal transition*. Sci Rep 2018.8, 14379

Stacklies W, et al. *pcaMethods--a bioconductor package providing PCA methods for incomplete data.* Bioinformatics, 2007 May 1;23(9):1164-7.

Stocum D, et al. *Regeneration of Epidermal Structures, Regenerative Biology and Medicine (Second Edition).* Academic Press, 2012, Pages 43-65, ISBN 9780123848604.

Takahashi S, et al. *Synergistic activation of endothelial nitric-oxide synthase (eNOS) by HSP90 and Akt: calcium-independent eNOS activation involves formation of an HSP90-Akt-CaM-bound eNOS complex*. J Biol Chem, 2003 Aug 15;278(33):30821-7.

Takeda U, et al. *Targeted disruption of dermatopontin causes abnormal collagen fibrillogenesis*. J Invest Dermatol, 2002 Sep;119(3):678-83.

Takeo M, et al. *Wound healing and skin regeneration.* Cold Spring Harbor perspectives in medicine vol. 5,1, 2015.

Tiede S, et al. *Endocrine controls of primary adult human stem cell biology: thyroid hormones stimulate keratin 15 expression, apoptosis, and differentiation in human hair follicle epithelial stem cells in situ and in vitro.* Eur J Cell Biol, 2010:89(10):769–77.

Tomic-Canic M, et al. *Nexus between epidermolysis bullosa and transcriptional regulation by thyroid hormone in epidermal keratinocytes.* Clin Transl Sci, 2008:1(1):45–9.

Tonnesen M, et al. *Angiogenesis in wound healing*. J Investig Dermatol Symp Proc, 2000 Dec;5(1):40-6.

Vermeulen T, et al. *Glutamine synthetase is essential for proliferation of fetal skin fibroblasts.* Arch Biochem Biophys, 2008 Oct 1;478(1):96-102.

Vinaik R, et al. *Regulation of glycolysis and the Warburg effect in wound healing.* JCI, 2020.

Vogel C, et al. *Insights into the regulation of protein abundance from proteomic and transcriptomic analyses*. Nat Rev Genet. 2012 Mar 13;13(4):227-32.

Wallin G, et al. *Expression of the thyroid hormone receptor, the oncogenes c-myc and H-ras, and the 90 kD heat shock protein in normal, hyperplastic, and neoplastic human thyroid tissue.* Thyroid. 1992.

Wang N, et al. *Activities of MSCs Derived from Transgenic Mice Seeded on ADM Scaffolds in Wound Healing and Assessment by Advanced Optical Techniques.* Cell Physiol Biochem, 2017;42(2):623-639.

Wang T, et al. *Mammalian Eps15 homology domain 1 potentiates angiogenesis of non-small cell lung cancer by regulating β2AR signaling.* J Exp Clin Cancer Res, 2019 Apr 25;38(1):174.

Webb DJ, et al. *A modified human alpha 2-macroglobulin derivative that binds tumor necrosis factor-alpha and interleukin-1 beta with high affinity in vitro and reverses lipopolysaccharide toxicity in vivo in mice*. Lab Invest, 1998 Aug;78(8):939-48.

Wright T, et al. *Changes in Northern Elephant Seal Skeletal Muscle Following Thirty Days of Fasting and Reduced Activity*. Front Physiol, 2020 Oct 6;11:564555.

Wright T, et al. *Changes in Northern Elephant Seal Skeletal Muscle Following Thirty Days of Fasting and Reduced Activity.* Frontiers in physiology, 2020.

Xie F, et al. *miRDeepFinder: a miRNA analysis tool for deep sequencing of plant small RNAs.* Plant Mol Biol, 2012 Jan 31.

Yang Y, et al. *MiR-152 Regulates Apoptosis and Triglyceride Production in MECs via Targeting ACAA2 and HSD17B12 Genes*. Sci Rep, 2018.

Yochem PK, et al. *Hematologic and serum biochemical profile of the northern elephant seal (Mirounga angustirostris): variation with age, sex, and season*. J Wildl Dis, 2008 Oct;44(4):911-21.

Zexin L, et al. *The Effect of Inflammation on the Formation of Thyroid Nodules*. International Journal of Endocrinology, 2020.

Zhang Y, et al. *Activation of PGK1 under hypoxic conditions promotes glycolysis and increases stem cell-like properties and the epithelial-mesenchymal transition in oral squamous cell carcinoma cells via the AKT signalling pathway*. Int J Oncol, 2020 Sep;57(3):743-755.

Zhou X, et al. *Ribosomal proteins: functions beyond the ribosome*. J Mol Cell Biol, 2015 Apr;7(2):92-104.

Zimova M, et al. *Function and underlying mechanisms of seasonal colour moulting in mammals and birds: what keeps them changing in a warming world?* Biol Rev Camb Philos Soc. 2018 Aug;93(3):1478-1498.